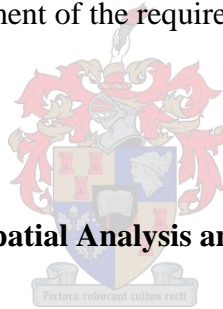


**REMOTE SENSING-BASED IDENTIFICATION AND MAPPING
OF SALINISED IRRIGATED LAND BETWEEN UPINGTON AND
KEIMOEES ALONG THE LOWER ORANGE RIVER, SOUTH
AFRICA**

by

Mashimbye Zama Eric

Thesis presented in partial fulfillment of the requirements for the degree:



Master of Science (in GIS for Spatial Analysis and Decision Making)

at the

University of Stellenbosch

Supervisor: Prof. HL Zietsman

APRIL 2005

AUTHORS' DECLARATION

I, the undersigned, hereby declare that the work contained in this thesis is my own original work and that I have not previously submitted it, in its entirety or in part, at any university for a degree.

Mashimbye ZE

Date

ABSTRACT

Salinisation is a major environmental hazard that reduces agricultural yields and degrades arable land. Two main categories of salinisation are: primary and secondary soil salinisation. While primary soil salinisation is caused by natural processes, secondary soil salinisation is caused by human factors. Incorrect irrigation practices are the major contributor to secondary soil salinisation. Because of low costs and less time that is associated with the use of remote sensing techniques, remote sensing data is used in this study to identify and map salinised irrigated land between Upington and Keimoes, Northern Cape Province, in South Africa.

The aim of this study is to evaluate the potential of digital aerial imagery in identifying salinised cultivated land. Two methods were used to realize this aim. The first method involved visually identifying salinised areas on NIR, and NDVI images and then digitizing them onscreen. In the second method, digital RGB mosaicked, stacked, and NDVI images were subjected to unsupervised image classification to identify salinised land. Soil samples randomly selected and analyzed for salinity were used to validate the results obtained from the analysis of aerial photographs.

Both techniques had difficulties in identifying salinised land because of their inability to differentiate salt induced stress from other forms of stress. Visual image analysis was relatively successful in identifying salinised land than unsupervised image classification. Visual image analysis correctly identified about 55% of salinised land while only about 25% was identified by unsupervised classification. The two techniques predict that an average of about 10% of irrigated land is affected by salinisation in the study area.

This study found that although visual analysis was time consuming and cannot differentiate salt induced stress from other forms; it is fairly possible to identify areas of crop stress using digital aerial imagery. Unsupervised classification was not successful in identifying areas of crop stress.

Key words: Remote sensing, normalized difference vegetation index (NDVI), image classification, salinisation, plant stress, orthorectification, mosaicking.

OPSOMMING

Versouting is 'n belangrike omgewingsrisiko wat landbou opbrengste verlaag en lei tot die agteruitgang van bewerkbare grond. Die twee hoof kategorieë van versouting is: primêre en sekondêre grondversouting. Terwyl primêre grondversouting natuurlik is, word sekondêre grondversouting veroorsaak deur menslike faktore. Verkeerde besproeiingspraktyke is die hooforsaak van sekondêre grondversouting. Lae kostes en min tyd wat geassosieër word met afstandswaarneming tegnieke het bygedra tot die gebruik van afstandswaarneming in die studie om versoute besproeiingsgrond te identifiseer en te karteer tussen Upington en Keimoes, in die Noord Kaap, Suid Afrika.

Die doelwit van die studie is om die potensiaal van digitale lugfoto's te evalueer vir versoute besproeiingsgrond. Twee metodes is gebruik om die doelwit te bereik, naamlik die visuele identifisering van versoute areas op NIR en NDVI beelde en dit was te lê op skerm. In die tweede metode is 'n digitale RGB mosaiek, gestapelde en NDVI beelde gebruik in 'n nie-gerigte beeldklassifikasie om versoute grond te identifiseer. Ewewoensig geselekteerde grondmonsters is ontleed vir versouting om die resultate verkry van die lugfotos te toets.

Beide tegnieke het moeilik versoute grond geïdentifiseer as gevolg van hul onvermoë om tussen sout verwante spanning en ander vorms van spanning te onderskei. Visuele beeld analise het ongeveer 55% van versoute grond korrek geïdentifiseer terwyl nie-gerigte klassifikasie ongeveer 25% korrek geklassifiseer het. Gemiddeld het beide tegnieke getoon dat 10% van besproeiingsgrond deur versouting beïnvloed is in die studie area.

Die studie het gevind dat alhoewel visuele analise tydrowend is en nie kan onderskei tussen sout verwante spanning en ander vorms van spanning nie, is dit nog steeds moontlik om oes verwante spanning met digitale lugfoto's te identifiseer. Nie-gerigte klassifikasie was nie suksesvol in die identifisering van oes verwante spanning nie.

ACKNOWLEDGEMENTS

I wish to express my sincere gratitude and appreciation to:

- Professor HL Zietsman for his guidance, support, arranging financial assistance, and for supplying me with all the data sets required for conducting this study.
- Mr. A Van Niekerk for allowing me to attend an introductory remote sensing course – this study would not have succeeded without it.
- My mentor at ARC, Ian Kotze for guidance and support.
- Mr BHA Schloms for his advice and knowledge of soil salinity.
- Geography department librarian, Ms Cronje for assistance in searching literature.
- Ms M Meise for editing the document.
- All staff and members of the Geography department for support.
- All friends and classmates for their support and encouragement.
- Wolfgang Luck for assistance in software and reading materials in remote sensing and soil science.
- My parents, brothers and sisters for assisting my family and me financially during the course of conducting this study.
- My parental uncle, Dr. KZ Nkuna and wife for their undying support, guidance, and motivation throughout the study.
- My wife, Basani for support and allowing me to leave her at home for the duration of this study.
- My children Thulani and Kurshell for their patience when I was not there to look after them during the course of the study.
- Almighty God for giving me inspiration and dedication to complete the study.

CONTENTS

	Page
AUTHOR'S DECLARATION.....	(ii)
ABSTRACT.....	(iii)
OPSOMMING.....	(iv)
ACKNOWLEDGEMENTS.....	(v)
ABBREVIATIONS AND ACRONYMS.....	(ix)
TABLES.....	(x)
FIGURES.....	(xi)
CHAPTER 1 THE PROBLEM OF SALINISATION.....	1
1.1 BACKGROUND.....	1
1.1.1 Introduction.....	1
1.1.2 Salinisation along the Orange River.....	1
1.1.3 Remote sensing and soil salinisation.....	2
1.2 PROBLEM STATEMENT.....	3
1.3 THE STUDY AREA.....	4
1.4 AIMS AND OBJECTIVES	6
1.5 DATA REQUIREMENTS.....	6
1.5.1 Digital aerial imagery.....	6
1.5.2 Orthophoto maps.....	7
1.5.3 Digital elevation models (DEMs).....	7
1.5.4 Soil samples.....	7
1.6 RESEARCH METHODOLOGY.....	9
1.7 RESEARCH FRAMEWORK.....	9
1.8 STRUCTURE OF THE THESIS.....	11
CHAPTER 2 REMOTE SENSING AND AGRICULTURE.....	12
2.1 INTRODUCTION.....	12
2.2 SALINISATION.....	14
2.2.1 Effects of salinisation on plants.....	14
2.2.2 Salinisation research.....	15
2.3 REMOTE SENSING.....	16
2.3.1 The electromagnetic spectrum.....	16
2.3.2 Remote sensing in agriculture.....	17
2.3.3 Remote sensing of irrigated land.....	18

2.3.3.1 Image classification.....	19
2.3.3.2 Vegetation indices.....	20
2.4 CONCLUSIONS.....	21
CHAPTER 3 DIGITAL IMAGE PROCESSING.....	22
3.1 INTRODUCTION.....	22
3.2 ORTHORECTIFICATION	22
3.3 IMAGE MOSAICKING	24
3.4 IMAGE STACKING.....	26
CHAPTER 4 IDENTIFICATION OF CULTIVATED LAND.....	28
4.1 INTRODUCTION.....	28
4.2 VISUAL INTERPRETATION.....	28
4.2.1 Manual classification of the mosaicked RGB image.....	28
4.2.2 Manual classification of the mosaicked NIR image.....	29
4.2.3 Manual classification of the stacked image.....	30
4.2.4 Manual classification of the NDVI image.....	31
4.3 DIGITAL IMAGE ANALYSIS.....	32
4.3.1 Unsupervised classification of the RGB mosaicked image.....	33
4.3.2 Unsupervised classification of the stacked image.....	34
4.3.3 Unsupervised classification of the NDVI image.....	35
4.4 ACCURACY ASSESSMENT.....	36
4.4.1 Manual image classification.....	37
4.4.2 Digital image classification.....	40
CHAPTER 5 IDENTIFICATION OF SALINISED LAND.....	44
5.1 INTRODUCTION.....	44
5.2 AIR PHOTO INTERPRETATION.....	44
5.2.1 Visual analysis of the NIR mosaicked image.....	45
5.2.2 Visual analysis of the NDVI image.....	46
5.3 DIGITAL IMAGE ANALYSIS.....	47
5.3.1 Unsupervised classification of the RGB mosaicked image.....	47
5.3.2 Unsupervised classification of the stacked image.....	48

5.3.3 Unsupervised classification of the NDVI image.....	49
5.4 FIELD VALIDATION.....	50
5.4.1 Visual image analysis.....	50
5.4.2 Digital image analysis.....	53
CHAPTER 6 SYNTHESIS.....	56
6.1 INTRODUCTION.....	56
6.2 FINDINGS OF THE STUDY	56
6.3 RECOMMENDATIONS AND DIRECTIONS FOR FURTHER STUDY...	57
REFERENCES.....	59

ABBREVIATIONS AND ACRONYMS

ANN - Artificial Neural Network

ARC - Agricultural Research Council

AVHRR - Advanced High Resolution Radiometer

CA - Consumer's Accuracy

DEM - Digital Elevation Model

EC – Electrical conductivity

ERTS – Earth Resource Satellites

FAO – Food and Agriculture Organization

GCP – Ground Control Point

IRS- Indian Remote Sensing Satellite

NASA –National Aeronautics and Space Administration

NDVI – Normalized Difference Vegetation Index

NIR – Near infrared

NOAA – National Oceanic Atmospheric Administration

PA – Producer's Accuracy

RGB – Red Green Blue

UNESCO – United Nations Educational, Scientific and Cultural Organization

WRC – Water Research Commission

TABLES

	Page
Table 2.1 The extent of salt-affected soils in the world.....	13
Table 4.1 Confusion matrix comparing cultivated land identified by manual classification of the RGB mosaicked image with ground truth data.....	38
Table 4.2 Confusion matrix comparing cultivated land identified by manual classification of the NIR image with ground truth data.....	39
Table 4.3 Confusion matrix comparing cultivated land identified by manual classification of the stacked image with ground truth data.....	39
Table 4.4 Confusion matrix comparing cultivated land identified by manual classification of the NDVI image with ground truth data.....	39
Table 4.5 Confusion matrix comparing cultivated land identified by unsupervised classification of the RGB mosaicked image with ground truth data..	41
Table 4.6 Confusion matrix comparing cultivated land identified by unsupervised classification of the stacked image with ground truth data.....	41
Table 4.7 Confusion matrix comparing cultivated land identified by unsupervised classification of the NDVI image with ground truth data.....	42
Table 5.1 Confusion matrix comparing potentially salinised land identified by visual analysis of the NIR mosaicked image with analyzed samples.....	52
Table 5.2 Confusion matrix comparing potentially salinised land identified by visual analysis of the NDVI image with analyzed samples	52
Table 5.3 Confusion matrix comparing potentially salinised land identified by unsupervised classification of the RGB image with analyzed samples.....	54
Table 5.4 Confusion matrix comparing potentially salinised land identified by unsupervised classification of the stacked image with analyzed samples ...	54
Table 5.5 Confusion matrix comparing potentially salinised land identified by unsupervised classification of the NDVI image with analyzed samples ...	55
Table 6.1 Corrected estimates of potentially salinised land.....	57

FIGURES

	Page
Figure 1.1 Location of the study area.....	5
Figure 1.2 Diagrammatical representation of the research design.....	10
Figure 2.1 Major divisions of the electromagnetic spectrum.....	17
Figure 3.1 Orthorectified RGB image.....	23
Figure 3.2 Orthorectified NIR image.....	24
Figure 3.3 Mosaicked RGB images covering the study area.....	25
Figure 3.4 Mosaicked NIR images covering the study area.....	26
Figure 3.5 Stacked image of the study area.....	27
Figure 4.1 Cultivated land demarcated from manual classification of the mosaicked RGB image.....	29
Figure 4.2 Cultivated land demarcated from manual classification of the NIR mosaicked image.....	20
Figure 4.3 Cultivated land demarcated from manual classification of the stacked image.....	31
Figure 4.4 Cultivated land demarcated from manual classification of the NDVI image.....	32
Figure 4.5 Cultivated land demarcated from unsupervised classification of the mosaicked RGB image.....	34
Figure 4.6 Cultivated land demarcated from unsupervised classification of the stacked image.....	35
Figure 4.7 Cultivated land demarcated from unsupervised classification of the NDVI image.....	36
Figure 4.8 Land use at field sample points.....	38
Figure 5.1 Salinised land identified by visual interpretation of the NIR mosaicked image.....	45
Figure 5.2 Salinised land identified by visual interpretation of the NDVI image.....	46
Figure 5.3 Salinised land identified by unsupervised classification of the RGB mosaicked image.....	48
Figure 5.4 Salinised land identified by unsupervised classification of the stacked image.....	49

Figure 5.5 Salinised land obtained from unsupervised classification of the NDVI image.....	50
Figure 5.6 Salinity at field sample points.....	51

CHAPTER 1: THE PROBLEM OF SALINISATION

1.1 BACKGROUND

1.1.1 Introduction

Soil salinisation is a major environmental hazard that causes decline in plant productivity and degradation of agricultural land, thus leading to losses in agricultural yields (Metternicht & Zink 2003; Wang, Wilson & Shannon 2002; Greiner 1998). Rowel (1994) and White (1997) define salinisation as the process by which salts accumulate in soils. This problem mostly occurs in soils of arid and semi-arid regions (Allison, Brown, Hayward, Richards, Berstein, Fireman, Pearson, Wilcox, Bower, Hatcher & Reeve 1969; Fitzpatric 1980; Rowel 1994) as these areas do not have enough rainfall to leach out the salts that accumulate in the soil. According to Allison et al. (1969), saline soils are practically non-existent in humid regions except when soil has been subjected to the influence of sea water in river deltas and low lying lands near the sea.

According to Metternicht & Zink (2003) and Szabolcs (1994), the global extent of primary salt-affected soils is about 955 million ha, with secondary salinisation affecting some 77 million hectares. Also, 58% of secondary salinised areas are concentrated in irrigated areas. Metternicht & Zink (2003) further state that nearly 20% of all irrigated land is salt-affected, and this proportion continues to increase in spite of considerable efforts to reclaim land. Careful monitoring of soil salinity is required to ensure sustainable land use and management.

1.1.2 Salinisation along the Orange River

The Northern Cape Province, South Africa, where the study area is situated is semi-arid. According to the Department of Water Affairs and Forestry (1999), the implementation of the Lesotho Highlands Water Project will lead to the reduction of the dilution effect of the water from Lesotho because a portion of the water will be directed to the Vaal River Catchment. This factor led to the study that was conducted by the Department of Water Affairs and Forestry along the Orange River to model the extent of salinisation in the area.

Despite insufficient data available to conduct the study at the time, the Department's study indicated that salts are being retained in irrigated areas. One of the recommendations of the study was that the question of salinisation be urgently studied in more detail. Constant monitoring of salinisation along the Orange River will serve to provide information on the spatial and temporal distribution of salts. Findings of the study will be used as an aid in the decision-making process for water allocation and development of the Catchment Management Plan in that area.

According to Lenney, Woodstock, Collins & Hamdy (1996), identifying soils with high salinity using remote sensing data has relied primarily on two methods. The first method involves identifying saline soils through quantitative assessment of bright salt-crusted soils or dark waterlogged fields (Everitt, Escobar, Gerbermann & Alanniz; Sharma & Bhargava; Dwivendi & Rao; Mishra; Joshi & Devi as quoted by Lenney et al. 1996). In the second method, the presence of salts is inferred by its effects on the spectral response of vegetation in imagery (Richardson, Gerbermann, Gausman & Cuellar; Everitt, Gerbermann & Cuellar; Wiegand, Everitt & Richardson; Wallace, Campbell, Wheaton & McFarlane in Lenney et al. 1996), and from hand-held radiometric measurements (Toth, Csillag, Micheli & Biehl in Lenney et al. 1996).

1.1.3 Remote sensing and soil salinisation

According to McNairn, Ellis, Van der Sanden, Hirose & Brown (2002), and Wang, Wilson & Shannon (2002), the vast acreage associated with the global agricultural resource base and the high costs and time needed to conduct field surveys make the cost of field surveys prohibitive. Also, McNairn et al. (2002) state that the challenge of monitoring the state of crops and soil is further complicated by their dynamic nature.

Studies conducted by Wiegand, Richardson, Escobar & Gerbermann (1991); Muchow, Robertson & Pengelly (1993); Jamieson, Martin, Francis & Wilson (1995); Casanova, Epema & Goudriaan (1998); Boegh, Soegaard, Broge, Hasager, Jensen, Schelde & Thomsen (2002); Wang, Wilson & Shannon (2002); McNairn et al. (2002), and Zhang, Liu & O'Neill (2002) have demonstrated that the state of crops or vegetation can be determined by investigating their spectral reflectance patterns.

Zhang, Liu & O'Neill (2002) are of the opinion that there has been a growing interest in using optical remote sensors for mapping and monitoring crop diseases and stress because of the advances in airplane and satellite technology. Because of the significance of these findings for crop and vegetation studies, and considering the low cost and shorter time required by the use of remote sensing technology, remote sensing has become an indispensable tool for studying agricultural resources and crop growing conditions (McNairn et al. 2002; Zhang, Liu & O'Neill 2002).

1.2 PROBLEM STATEMENT

Rowel (1994) and White (1997) state that all irrigation water contains some amount of salts. According to White (1997), salts accumulate in soils under irrigation because crops take up little of this salt, e.g. NaCl (about one tenth) and transpire nearly all of the water. While the salinity of the water in the Orange River has been relatively low (Department of Water Affairs and Forestry 1999; Schloms 2002 [*Pers comm*]), because most of the water originates in the high rainfall area of Lesotho where the geology brings about water of generally low salt concentration, salts may accumulate as a result of irrigation over the long term. Another problem that contributes to salinisation is water logging that occurs at local depressions created by filled old drainage channels of the river. Salts accumulate in these areas when the water evaporates (White 1997).

Although the literature points that several remote sensing data sets are available for use in identifying soils with high salt content, the use of remote sensing in studying salinisation in South Africa is still lacking. This was revealed by unavailability of literature on the use of remote sensing techniques in studying salinised land in South Africa. Although it is possible to study and map salinised land by studying the reflectance patterns of the soil, this study uses the reflectance patterns of plants in salinised land to identify salinised areas. The reason for this choice is that the potentially affected areas are under permanent cultivation and studies have shown that salinisation alters the reflectance patterns of plants.

Reversing the effects of salinisation can be a very expensive practice, so constant monitoring of the state of the soils is essential. This will help in diagnosing the problem before it is too severe and then taking steps to avert the situation.

1.3 THE STUDY AREA

The study area selected is located in the Northern Cape Province, South Africa, along the lower Orange River, between Keimoes and Upington. The total surface area of the study region is 4130 hectares of which 2107 hectares are cultivated agricultural land. Orchards and vineyards are a major part of land use in the study area. The average maximum daily temperatures are 35°C and 20°C in summer and winter respectively and this area has an average precipitation of about 25mm in summer and 5mm in winter (South African Weather Service 1991). Figure 1.1 shows the location of the study area. On the study area map Upington is situated on the upper side in a northeasterly direction and Keimoes is found further down in a southwesterly direction.

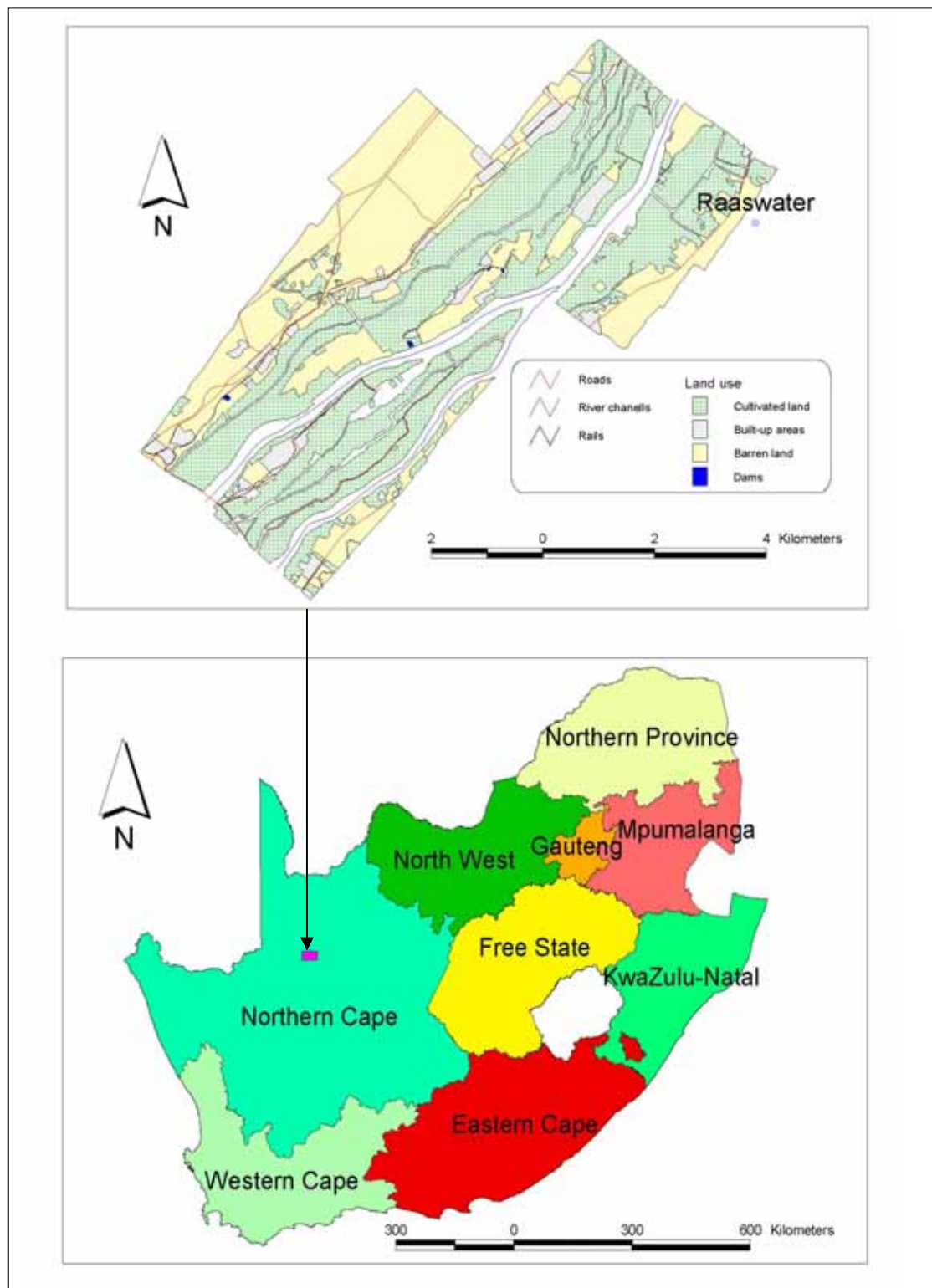


Figure 1.1 Location of the study area

1.4 AIMS AND OBJECTIVES

Studies by Penuelas, Isla, Filella & Araus (1997); Katerji, Van Hoorn, Hamdy & Mastrorilli (1998); Wang, Shannon & Grieve (2001), and Wang, Wilson & Shannon (2002) succeeded in showing how saline conditions alter the reflectance patterns of plants grown under these conditions. These findings on remote sensing and the benefits in low costs, less time needed to conduct the study, and the objectivity associated with the use of remote sensing constitute sufficient reason to justify the use of the technology in studying crop conditions.

The overall aim of the study is to evaluate the potential of visible and near infrared digital aerial imagery in the identification of salinised-cultivated land. The following objectives will help realise the aim stated above:

1. Identify cultivated from non-cultivated land in the study area;
2. Identify and map areas in which crops show stress;
3. Evaluate the extent of the problem of salinisation in the study area;
4. Evaluate the success of the technique in identifying salinised land.

1.5 DATA REQUIREMENTS

The data that were used to conduct this study comprise digital aerial images, orthophoto maps, digital elevation models (DEMs), and field data. Each of these data sets is briefly described below.

1.5.1 Digital aerial imagery

Digital aerial images were acquired in December 2002 by the company Emoyeni (Somerset West). The images overlap by 60% in the flight direction with a 30% side lap. The focal length of the camera was 50mm and the average flight height was about 3960 meters. The resolution of the images is 4079 rows x 4080 columns and each pixel represents approximately 0,65m on the ground. The scale of the images is 1:70000.

Two sets of imagery were acquired. The spectral channels of the colour images consist of the red, green, and blue (RGB) bands, whereas the second set of images were black and white near infrared (NIR). The study area is covered by 20 RGB and 20 NIR images. Because the two sets of images were captured separately, they could

not cover the same areas on some portions of the study area, more especially images at the edges. Vegetated areas appeared in a bright white colour on NIR images while non-vegetated areas were dark. On RGB images, vegetated areas appeared green while non-vegetated areas were greyish in colour.

1.5.2 Orthophoto maps

Digital orthophoto maps were obtained from the Chief Directorate of Surveys and Mapping in Mowbray. The orthophoto maps were georeferenced to the South African LO co-ordinate system and used as a backdrop for collecting ground control points when rectifying digital aerial images. The orthophoto maps that covered the study area are 2821CA12, 2821CA13, 2821CA17 and 2821CA18 and they were captured in 2001.

1.5.3 Digital Elevation Models (DEMs)

Digital elevation models (DEMs) covering the study area were obtained from the Chief Directorate of Surveys and Mapping in Mowbray. The resolution of the DEMs was 20 meters. The DEMs were used as a source of elevation data when orthorectifying digital aerial images using the Orthobase module of ERDAS Imagine Software.

1.5.4 Soil samples

Considering the time available to conduct this study, and the high costs of laboratory analysis, the findings of this study were validated by 24 samples, which were collected for the broader study conducted along the Orange River. The broader study of which this one formed a sub-component was undertaken for the Water Research Commission (WRC) by Mrs T.Volschenk, ARC/Infruitek, Prof. HL Zietsman, Department of Geography and Environmental Studies, and Prof. M Fey, Department of Soil Science, University of Stellenbosch. The study was aimed at determining the seriousness of the problem of salinisation along the Orange River.

Of the 200 randomly and proportionally selected samples from twelve sampled blocks for the broader project along the Orange River, 24 samples occurred in the study area for this project. For all areas identified as salinised, control soil samples were collected in non-salinised plots adjacent to plots identified as salinised. Thus of the 24

samples, 12 were collected from non-salinised plots adjacent to those identified as salinised.

The geographical co-ordinates of the selected sites were extracted and provided to the field survey team for locating the sites using a GPS. To expedite the location of these sites in the field the field team was given a set of twelve A1 sized colour maps showing the mosaicked RGB images with a graticule and an overlay of the selected sample sites. This set of twelve maps was accompanied by similar data in TIFF and Shape file formats on a Notebook computer, using ESRI's ArcExplorer software, so that the field team could zoom into any area and determine exactly where any particular soil sample point was located.

The field teams were also instructed to note the land cover type of the sample sites as well as any observations on the soil conditions or factors that could assist in explaining observed patterns. These observations were captured on the database and used in an assessment of the accuracy of the aerial photographic techniques employed in identifying areas showing some form of vegetation stress. Information on land-cover types on the sample sites was used to determine classification accuracies.

Soil samples were taken to determine the total salt concentration by measuring the electrical conductivity of the saturated soil water extract (EC_e) and the soluble cations and anions. Soils were sampled at the following depths: 0 to 300mm, 300 to 600mm and 600 to 900mm. Soils were dried, sieved, and saturated paste extracts made (Richards 1954). The saturation percentage, PH, and EC of the saturated extract (EC_e, dS/m) were determined. Soluble cations (Na, K, Ca, Mg) in the saturated extract were determined using an inductive coupled plasma atomic emission spectrometer (Liberty 200 ICP, Varian Australia Pty Ltd, Australia) and anions (Cl, SO₄) according to Richards (1954). The soils were classed for salinity status according to the profile mean EC_e and soils were considered saline if the EC_e was equal to or exceeded 0,75 dS/m, which is the salinity threshold value beyond which a decrease in yield for grapes is expected (Moolman, De Clerg, Wessels, Meiri & Moolman 1999).

1.6 RESEARCH METHODOLOGY

In order to realise the overall aim of the study, the following procedures were executed:

1. Orthorectification of digital aerial images to correct for terrain displacement on the images,
2. Digital image mosaicking of each of the two sets of RGB and NIR images to produce images of each set that cover the whole study area,
3. Stacking the NIR and RGB mosaicked images to produce a four-band image that can be used for computing the NDVI image,
4. Manual and digital image classification to identify irrigated land,
5. Visual and digital image analysis to identify and map potentially salinised land,
6. Conducting accuracy assessments to determine the success of manual and digital image classification techniques,
7. Validation of results using soil samples obtained from field surveys.

1.7 RESEARCH FRAMEWORK

The research design depicted in Figure 1.2 shows the sequence of steps followed in this study to realise the aim and objectives. The study consists of the following main elements:

1. Review of the relevant literature,
2. Manual and digital image analysis for the identification of irrigated land, and potentially salinised areas,
3. Overall findings of the study.

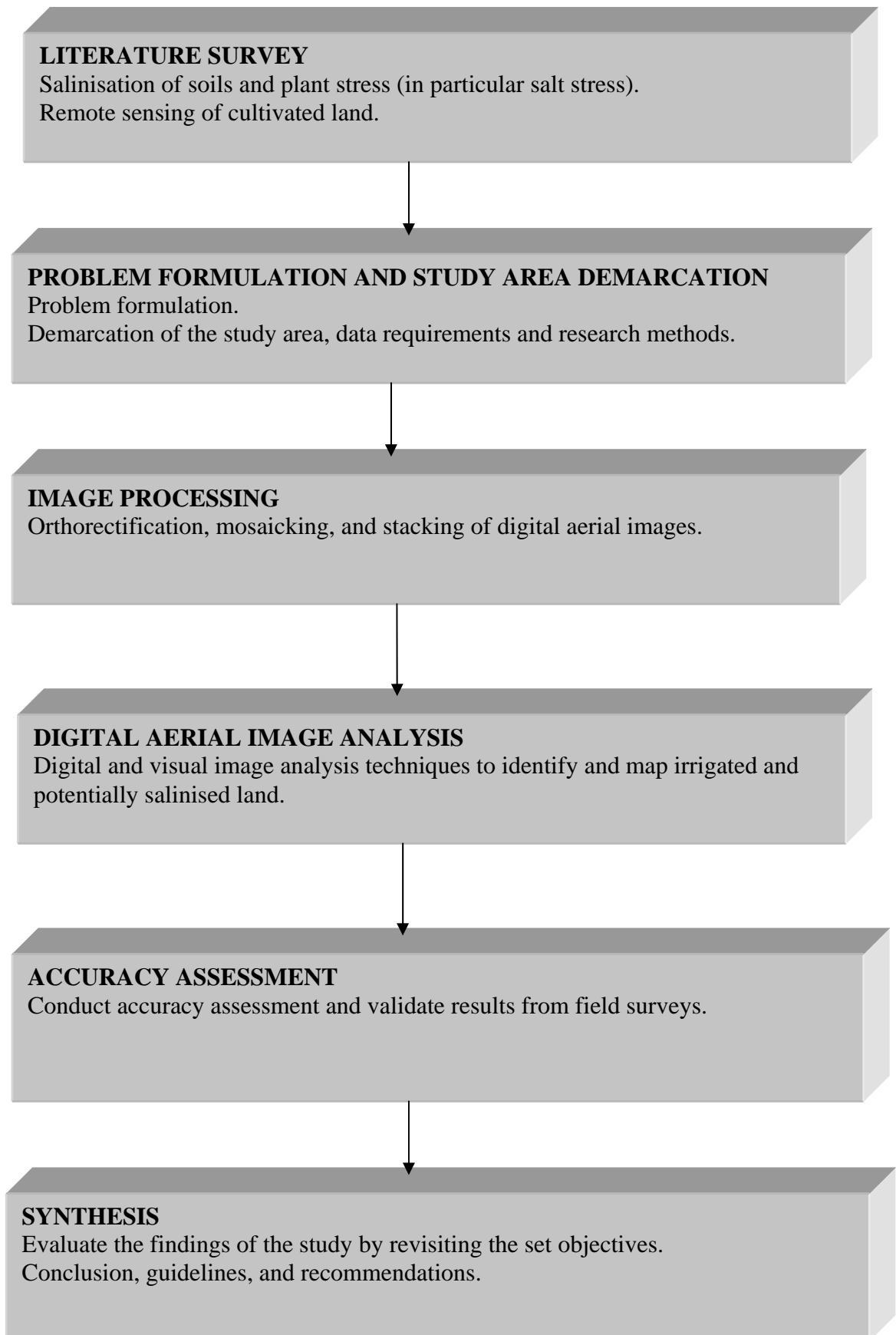


Figure 1.2 Diagrammatical representation of the research design

The literature survey involved a review of the literature to provide the theoretical background to the study. Literature consulted covered salinisation, remote sensing and the use of remote sensing techniques in studying crop and vegetation stress. Particular attention was paid to studies that focused on crop and vegetation salt stress.

Visual and digital image analysis involved manual and digital image classification of the digital aerial images to identify irrigated, potentially salinised land. Accuracy assessments were conducted on the classified images to determine the success of the classification techniques. Chemical analysis of soil samples obtained from field surveys were then incorporated to verify salinity areas derived from remote sensing mapping.

Overall findings of the study are evaluated at the end of the study to determine the success of the study in identifying salinised land. Conclusions are then drawn and recommendations made.

1.8 STRUCTURE OF THE THESIS

In this report, Chapter 1 presents an introduction to salinisation and the use of remote sensing techniques in studying salinised land. The problem statement is then defined, followed by aims and objectives, and demarcation of the study area. Data needs and research methods are also explained in this first chapter. Chapter 2 deals with the theoretical background on salinisation and remote sensing. Chapter 3 covers the image processing techniques conducted on the images to prepare them for analysis. The identification of irrigated land in the study area is explained in Chapter 4, followed by the identification and mapping of potentially salinised land in Chapter 5. Chapter 6 presents the findings of the study. Conclusions and recommendations are made in this last chapter.

In the following chapter, the theoretical background of the study is outlined.

CHAPTER 2: REMOTE SENSING AND AGRICULTURE

2.1 INTRODUCTION

The review of the literature in this chapter provides a theoretical base for the identification and mapping of salinised-irrigated land. The first part of the chapter deals with salinisation of soils, the causes of salinisation, effects on plant growth, and research on salinisation. The remaining parts of the chapter consider literature on remote sensing of cultivated land. The use of remote sensing in studying agricultural land, particularly the use of the technology in isolating irrigated from non-irrigated land, and the use of the technology in studying plant stress are reviewed.

According to Ammissah-Arthur & Miller (2002), the greatest problem facing the world today is that of chronic hunger, more especially in developing countries. Ammissah-Arthur & Miller (2002) further state that Africa has an annual population growth of 2,38% compared to the global rate of 1,33% and that, although it accounts for only 10% of the world population, it produces too little to feed its people. In order to meet the demands of the growing population, tremendous pressure is being put on finite natural resources to provide for the substantial production of food crops, water and energy (Zietsman, Vlok & Nel 1998). While farmers and agricultural managers strive to increase production while cutting costs, they should also guard against damaging the environment. To employ optimised management techniques, highly detailed information on the status of the soils, conditions of crops and manifestation of diseases is essential.

Greiner (1998); Utset & Borroto (2001); Slavich, Petterson & Griffin (2002), and Cuartero & Fernandez-Munoz (1998) state that incorrect methods of irrigation lead to salinisation and pose a threat to the sustainability of irrigation agriculture. As outlined in Table 2.1, no continent on the globe is free from salt-affected soils. Estimates of the Food and Agriculture Organisation (FAO) and United Nations Educational, Scientific and Cultural Organisation (UNESCO) reveal that as many as half of the existing irrigation systems of the world are affected by salinisation, alkalisation and water logging. About ten million hectares of arable land are abandoned annually because of the negative effects of salinity due to irrigation (Szabolcs 1994). Salinisation resulting

from the effects of human activities (irrigation being the major contributor) is adding to the 954,8 million hectares of land already salinised through natural processes (see Table 2.1).

Table 2.1 The extent of salt-affected soils in the world

Source: Szabolcs, 1994:6

Continent	Area (million ha)	% of Total
North America	15,7	1,6
Mexico and Central America	2,0	0,2
South America	129,2	13,5
Africa	80,5	8,4
South Asia	87,6	9,2
North and Central Asia	211,7	22,2
Southeast Asia	20,0	2,1
Australia	357,3	37,4
Europe	50,8	5,3
TOTAL	954,8	100

Traditionally, field survey methods were commonly used in monitoring agricultural crops and the condition of soils. McNairn et al. (2002) argue that the vast acreage that is associated with the global agricultural resource base makes the use of field surveying methods prohibitive because of high costs and the time that is associated with them. Also, the challenge of monitoring the state of crops is further complicated by their dynamic nature. Recent developments in remote sensing technology have brought new airborne and satellite sensors with high resolution that also provide continuous availability of remote sensing data. According to Liu & Kogan (2002), remote sensing data provide high-quality spatial and temporal information about land surface features, including the behaviour of agricultural crops and cumulative environmental crop growing conditions. These developments make remote sensing the most economical and convenient way of obtaining information about the environment and the conditions of soils and agricultural crops.

2.2 SALINISATION

Salinisation, the process whereby salts accumulate in soils, is the world's oldest soil-pollution problem (Rowel 1994). Literature on salinisation indicates that it occurs in soils of arid and semi-arid regions (Allison et al. 1969; Fitzpatric 1980; Rowel 1994). As stated by Allison et al. (1969), saline soils are practically non-existent in humid regions except when the soil has been subjected to the effects of seawater in river deltas and low-lying lands near the sea. Restricted drainage is a factor that usually contributes to the salinisation of soils (Allison et al. 1969).

Allison et al. (1969), and Szabolcs (1994) identify two major categories of salt-affected soils:

- (i) Primary soil salinisation – salt-affected soils that develop as a result of natural processes and
- (ii) Secondary soil salinisation - soils that have been salinised as a result of human activities.

Irrigation and human activities other than irrigation (e.g. deforestation, overgrazing, accumulation of air-borne or water-borne salts etc.) are identified as the causes of secondary soil salinisation. But according to Lenney, Woodstock, Collins & Hamdy (1996); Smets, Kuper, Van Dam, & Feddes (1997); Wienhold & Trooien (1998); Katerji et al. (1998); Utset & Borroto (2001), and Slavich, Petterson & Griffin (2002), incorrect irrigation practices constitute the major contributor to secondary soil salinisation. According to Szabolcs (1994) and White (1997), it is estimated that more than half of the irrigated land of the world have been affected by salinisation and the problem is increasing rather than decreasing.

2.2.1 Effects of salinisation on plants

All soils contain a considerable mixture of salts, some of which are essential for plant growth. When the concentration of salts becomes excessive, plant growth is suppressed and productivity of plants is reduced (Francis & Maas 1994; Greiner 1998; Wang et al. 2002). The suppression increases as the concentration of the salt increases until the plant dies (Francis & Maas 1994).

The fact that crops react differently to salinisation of different levels under different conditions has been clearly accounted for in the literature (Maas & Hoffman 1977; Francis & Maas 1994; Dudley 1994; Katerji et al. 1998; Armour & Viljoen 2000; Asch & Wopereis 2001; Katerji, Van Hoorn, Hamdy & Mastrorilli 2001). Maas & Hoffman (1977) maintain that the response of plants to different levels of salts is dependent on plant factors, type of soil, water and environmental factors.

Research and experiments conducted on a variety of plants and crop cultivars reveal different responses of plants to salinisation. Although all plants are subject to stunting, the tolerance threshold varies widely among different crops. Salinisation decreases the amount of water available to the plant (by decreasing the osmotic pressure), thus leading to leaf burn and defoliation (Thorburn, Walker & Jolly 1995). Salinisation can decrease growth and net photosynthesis in plants and alters the reflectance of electromagnetic radiation by plants (Penuelas, Isla, Filela & Araus 1997; Jamieson et al. 1995; Wang et al. 2002). This impaired photosynthesis leads to reduction in biomass and yield of plants.

A study conducted by Cuartero & Fernandez-Munoz (1998) found that salinisation reduces tomato seed germination. According to William & Mathews (1990), although grapes are moderately resistant to salinity, severe saline conditions inhibit growth and delay ripening.

2.2.2 Salinisation research

Millions of hectares of irrigated land are lost yearly and great losses are incurred in agricultural production all over the world because of salinisation. As a result, a variety of disciplines have focused on the problem. A wide range of research themes has been covered in the literature. These include studies on plant salt tolerance, salt stress and plant productivity, plant radiation reflectance under saline conditions, salt infiltration rates, irrigation and salinity, etc. (Maas & Hoffman 1977; Katerji, Van Hoorn, Karam & Mastrorilli 1996; Katerji et al. 1998; Wang, Shannon & Grieve 2001; Katerji et al. 2001; Mahmood, Morris, Collopy & Slavich 2001; Asch & Wopereis 2001; Slavich, Petterson & Griffin 2002; Wang, Wilson & Shannon 2002; Wang, Poss, Donovan, Shannon & Lesch 2002)

Thorburn, Walker and Jolly (1995) developed an analytical model, based on unsaturated zone water and solute balances, to describe the uptake of saline groundwater by plants in dry regions. Their study was conducted in Australia in 1995. This study found that groundwater depth and salinity were the main controls on the uptake of groundwater, while soil properties appeared to have a lesser effect. The model showed that uptake of groundwater would result in the complete salinisation of the soil profile within 4 to 30 years at sites they studied, unless salts were leached by rainfall or floodwater. Penuelas et al. (1997) studied the effects of the soil salinity gradient on spectral reflectance of genotypes of barley to determine the efficacy of reflectance as a tool for assessing the response of barley to salinity. Using the normalised difference vegetation index (NDVI) and the Water Index (WI), they found that near-infrared reflectance of barley decreased and visible reflectance increased in response to increasing salinity.

2.3 REMOTE SENSING

Campbell (1996: 5) defines remote sensing as the practice of deriving information about the earth's land and water surfaces using images acquired from an overhead perspective, using the electromagnetic spectrum reflected or emitted from the earth's surface. While other authors have their own ways of defining remote sensing, they all centre on the observation of features on the surface of the earth by recording the behaviour of electromagnetic radiation when it interacts with objects on the surface of the earth. Central to the practice of remote sensing is an understanding of the electromagnetic spectrum and how it interacts with objects on the surface of the earth.

2.3.1 The electromagnetic spectrum

According to Campbell (1996), all objects except those at absolute zero temperature (0 Kelvin or -273°C) emit electromagnetic energy, while others reflect radiation from other objects. A full range of the electromagnetic energy is radiated towards the earth from the sun (Campbell 2002). This range of energy is called the electromagnetic spectrum. According to Lindgren (1985), the electromagnetic spectrum is the arrangement of electromagnetic radiation according to wavelength or frequency. Campbell (1996) maintains that, while electromagnetic energy can be classified according to wavelength or frequency, the most commonly used method of classifying electromagnetic energy is by wavelength.

Arbitrarily, the electromagnetic spectrum can be divided into regions according to wavelengths. Figure 2.1 shows the various divisions of the electromagnetic spectrum. The waves with the shortest wavelengths are the gamma rays ($< 0,03\text{nm}$), followed by the X rays ($0,03 - 300\text{nm}$), ultraviolet ($0,30 - 0,38\mu\text{m}$), visible ($0,038 - 0,72\mu\text{m}$), infrared ($0,72 - 1\text{mm}$), microwaves ($1 - 300\text{mm}$) and radio waves ($> 30\text{cm}$). The portion of the electromagnetic spectrum that is applicable to remote sensing ranges between the ultraviolet ($0.3\mu\text{m}$) and the microwave ($0.8\mu\text{m}$) regions (Lindgren 1985, Campbell 1996).

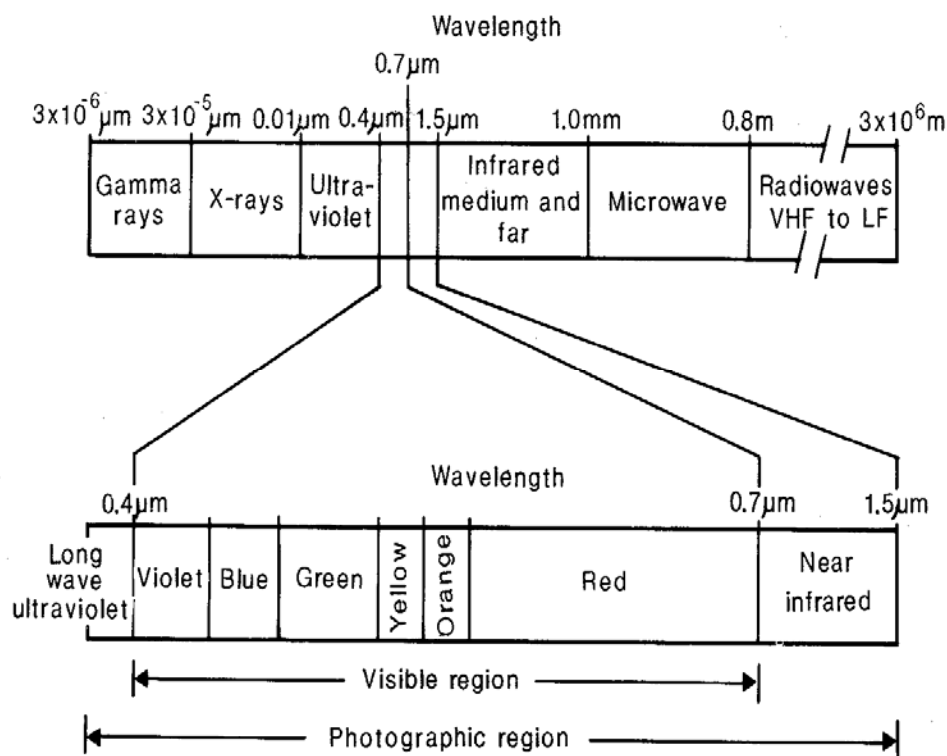


Figure 2.1 Major divisions of the electromagnetic spectrum

Source: Lindgren, 1985: 4

2.3.2 Remote sensing in agriculture

Lunetta (1999) argues that the launching of the first earth resource satellites (ERTS-1) in 1972 by NASA saw the recognition of the utility of space-borne remote-sensor platforms and their potential for long-term environmental monitoring. Various satellites carrying sensors of different resolutions have been launched since 1972 to

assist in studying environmental problems viz. land degradation (e.g. vegetation cover, erosion, salinity, urbanisation etc.), water pollution and air pollution.

While the application of remote sensing in agriculture has attracted the attention of many countries for many years (Hal-Konyves 1988), the resolution of the data was a deterring factor. Zietsman, Vlok & Nel (1998) and Allan (1990) argue that applications of remote sensing in agriculture require high spatial, radiometric, temporal, and spectral resolution. Research has, however, led to the development of new sensors with higher resolution. These developments in remote sensing technology have brought many applications of the technology to agricultural studies. These applications include crop and stress studies, diseases and weed infestation, monitoring the status of agricultural crops, determining biomass, yield focusing, precision farming, etc. (Lenney et al. 1996; Lelong, Pinet & Poilve 1998; Blackmer & White 1998; Lanjeri, Melia & Segarra 2001; McNairn et al. 2002; Liu 2002; Boegh et al. 2002; Haboudane, Miller, Tremblay, Zarco-Tejada & Dextraze 2002; Dabrowska-Zielinska, Kogan, Ciolkosz, Gruszczynska & Kowalik 2002; Goel, Prasher, Landry, Patel, Bonnel, Viau & Miller 2003, Johnson, Roczen, Youkhana, Nemani & Bosch 2003).

2.3.3 Remote sensing of irrigated land

Remote sensing has made a significant contribution to vegetation mapping and monitoring through the relationship between spectral reflectance and vegetation greenness (Lewis 1998). With every object having its own unique way of reacting with the electromagnetic spectrum, spectral reflectance (the ratio of radiant energy within specific wavelengths reflected by a body to the incident energy within the same wavelength) can be used to distinguish objects from one another (Mulders 1987; Campbell 1996). According to Hal-Konyves (1988), spectral measurements on a single occasion may not be sufficient for the purpose of discrimination and crop classification. Various techniques can be used to enhance identification of irrigated vegetation from non-irrigated vegetation. These techniques include image classification, and vegetation indices. Each of these techniques is discussed in the following subsections.

2.3.3.1 Image classification

Image classification is the process of assigning pixels to classes. Campbell (1996) state that image classification forms an important part of the field of remote sensing, image analysis and pattern recognition. Several techniques are available for performing classification of images. These include supervised classification, unsupervised classification, fuzzy clustering, artificial neural networks, layered classification. Although only unsupervised classification was used in this study, each of these techniques is briefly explained in the following paragraphs. This will serve to clarify the differences and basic requirements of some of these techniques.

Supervised classification involves the use of known reflectance, called training areas to classify digital images. Training areas, which are areas of homogeneous land cover, are used to assist the computer to classify digital images. In contrast to supervised classification, unsupervised classification does not make use of training data to classify digital images. This technique uses algorithms to group pixels in an image into clusters with similar reflectance properties.

According to Campbell (2002), fuzzy clustering attempts to assign pixels to a single discrete class. A fuzzy classifier assigns membership to pixels based upon a membership function. These membership functions for classes are determined by either general relationships or definitions of rules describing the relationship between data and classes. The output of a fuzzy classification is likely to form an image that shows varied levels of membership for specific classes.

Artificial neural networks (ANNs) are computer programs that are designed to simulate human learning processes through establishment and reinforcement of linkages between input data and output data (Campbell 2002). They are designed using less severe statistical assumptions than many other classifiers. ANNs have been found to be accurate in the classification of remotely sensed data.

Layered classification refers to the use of a hierarchical process in which two or more steps form the basis of classification (Campbell 2002). In this classification, subsets of data are classified in a series of separate steps by applying different forms of information in its most effective context. This classification method can only be used

if the classification logic can be structured in a way that minimizes errors at the upper level of the decision tree.

2.3.3.2 Vegetation indices

To assist in the study of vegetation by remote sensing, a number of vegetation indices have been developed. Vegetation indices are linear or non-linear combinations of reflectance acquired in several bands. They are based on digital brightness values and attempt to measure biomass. Research has found that in living vegetation there is a strong absorption of red light by chlorophyll and a strong reflection of infrared radiation by chlorophyll (Wang, Shannon & Grieve 2001; Campbell 2002). This relationship raises the measurement values of vegetation indices for healthy vegetation and makes it possible to distinguish water, bare soil and stressed vegetation from healthy vegetation.

Although several vegetation indices are available for vegetation studies, the normalised difference vegetation index (NDVI) is the most commonly used. NDVI is computed by the following formula:

$NDVI = \frac{IR - R}{IR + R}$, where IR is the amount of infrared reflection and R is the amount of red light reflection.

Campbell (2002) warns that, although vegetation indices are powerful tools in studying vegetation, care should be taken when using them because they can be influenced by the viewing angle, soil background, and differences in row direction and spacing in the case of agricultural crops.

Uchida (1997) used the normalised difference vegetation index (NDVI) in a temporal analysis of agricultural land use in the semi-arid tropics of India, using IRS data in 1997. The NDVI of cropped areas was found to be higher than that of forested areas. In 1995, Hooda and Dye used NDVI to identify and map irrigated vegetation. They used data from the pathfinder AVHRR from the NOAA11 satellite. NDVI was calculated from atmospherically corrected surface reflectance from visible and NIR channels. They calculated monthly and seasonal NDVI averages. NDVI values of irrigated vegetation should be less dependent on climate, so they used this difference to separate irrigated from non-irrigated vegetation.

2.4 CONCLUSIONS

The literature reveals that salinisation is an environmental hazard that is increasing despite negative experiences. This soil condition has been proved to negatively affect the production of most crops thus posing a threat to the sustainability of irrigation agriculture. Amongst other causes of secondary soil salinisation, irrigation is identified as the main contributor. While the traditional field survey method of studying soil salinity has been found to be time consuming and expensive, remote sensing technologies require less time and are relatively cost effective in studying agricultural problems (salinisation included).

The current state of remote sensing studies and the use of the technology have proved to be very useful in the solution of a wide variety of environmental problems, including agricultural problems as outlined in this chapter. The application of the technology in addressing agricultural problems is the result of the rapid development the technology has undergone. This was not the case a few decades ago.

The variety of agricultural problems ranging from state of soils (e.g. salinity, soil wetness, etc.) to detection of crop stress and forecasting of yields, that can be addressed by the use of remote sensing technology is extensively covered in the literature. Studies have revealed the relationships that occur between the conditions of plants and alterations that occur in the reflectance characteristics of specific parts of the electromagnetic spectrum. These findings make remote sensing an indispensable tool in the study of agricultural problems.

The chapter that follows discusses digital image processing techniques conducted on the imagery.

CHAPTER 3: DIGITAL IMAGE PROCESSING

3.1 INRODUCTION

Image processing entails operations that are carried out on the imagery to prepare them for analysis. According to Campbell (2002), image pre-processing changes data and the change is assumed to be beneficial. Orthorectification and image mosaicking are the two image pre-processing techniques that the images were subjected to. Firstly, the images were orthorectified and thereafter mosaicked to produce an image covering the whole study area. Because the RGB and NIR images were captured during separate overflights, the mosaicked RGB and NIR images were stacked to produce an image with four bands. An NDVI image was computed from this four-band image.

3.2 ORTHORECTIFICATION

According to ERDAS (2002), orthorectification is a form of rectification that corrects for terrain displacement and should be used if there is a DEM of the study area. The process of orthorectification takes the raw digital images and applies a DEM and triangulation results to create orthorectified images. It is based on collinearity equations that can be derived by using 3D ground control points (GCPs). Orthorectification of the aerial images for this study was conducted using the ORTHOBASE module of the ERDAS Imagine version 8.6.

The ERDAS Imagine Orthobase module uses a self-calibrating bundle block adjustment method in its triangulation, thereby determining the relationship between overlapping images and their internal geometry. Images can be orthorectified individually or in multiples in a block. The process of orthorectification in Orthobase requires a DEM, ground control points, tie points and camera calibration information. The two sets of digital imagery (NIR and RGB imagery) were orthorectified separately as they were captured during separate overflights.

Ground control points were collected manually using the 1: 10 000 digital orthophoto maps as backdrops. The literature shows that it is possible to triangulate a project with only three or four GCPs, but it is important to use more GCPs in order to improve spatial accuracy. A minimum of six GCPs were collected for each image in the block,

most of them in the overlapping areas of the images and distributed throughout the images. Because the NIR had shadows, GCPs collected on them were not very accurate; corners of some buildings and other structures were not easy to locate accurately on these images. This kind of problem was not present in the RGB images.

Automatic tie point generation created many errors and a decision to collect tie points manually was taken. In both projects, collecting too many tie points resulted in a higher RMS error. The RGB and NIR images were triangulated with total RMS errors of 0,64 and 0,88 of a pixel respectively. The much higher RMS error for triangulating NIR images could be attributed to the poor GCPs collected on these images because of shadows. Figure 3.1 and 3.2 show samples of orthorectified RGB and NIR images respectively.

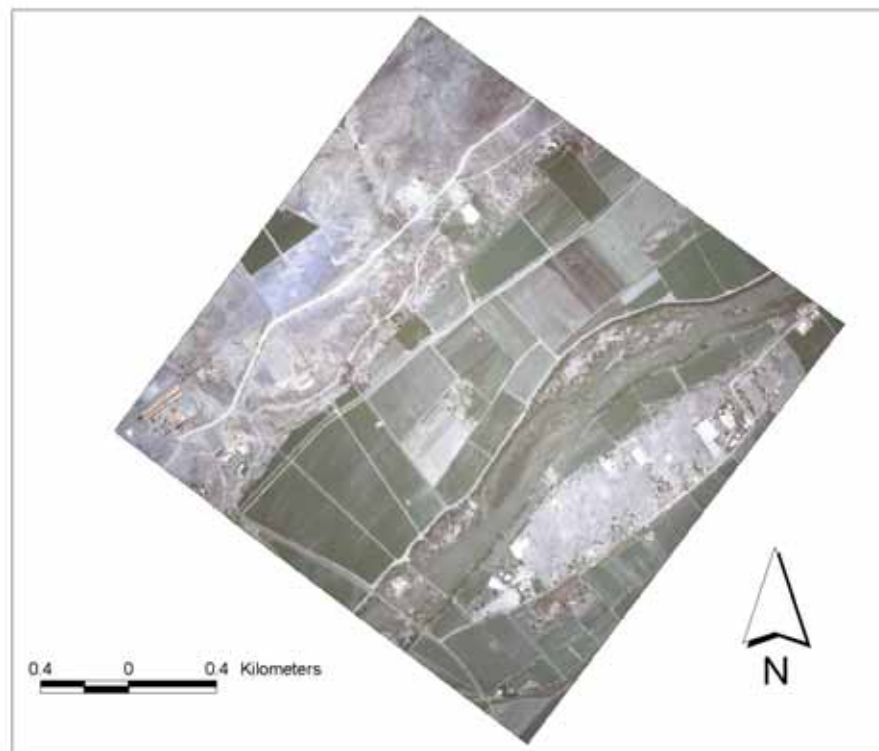


Figure 3.1 Orthorectified RGB image

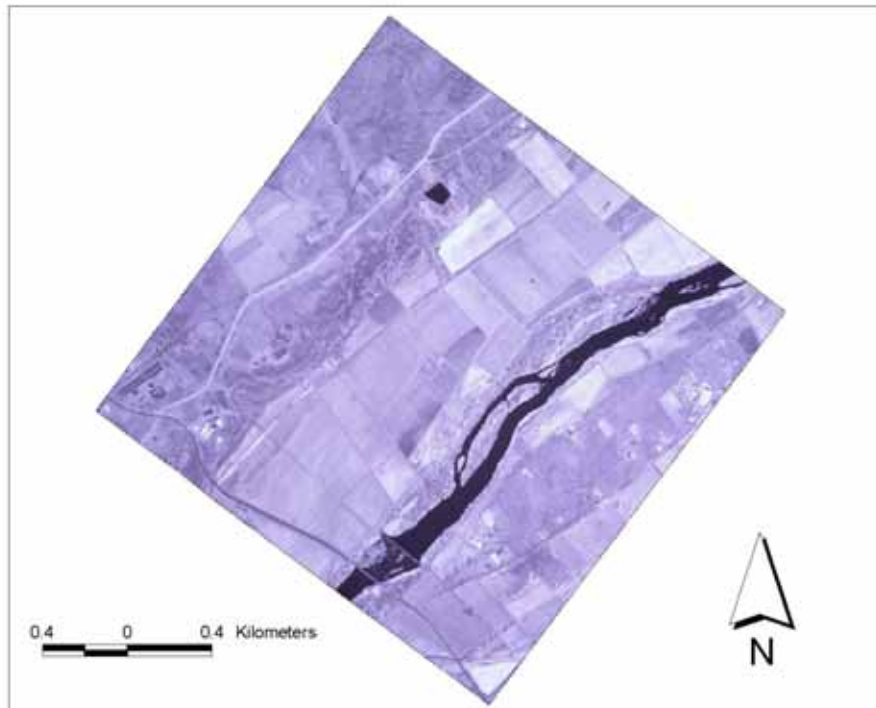


Figure 3.2 Orthorectified NIR image

3.3 IMAGE MOSAICKING

Mosaicking is the combination of many images to produce one large image of an area. Aerial photographs are usually a common source for creating image mosaics. According to ERDAS (2002), input images must all contain map and projection information, although they need not be in the same projection or have the same cell sizes. According to Yehuda & Brand (1998), geometric distortions added during the process of orthorectification vary for different photos. This difference may result in the features appearing in two map plane coordinates on the two adjacent orthorectified images created from both photographs. Yehuda & Brand (1998) further state that geometric differences between adjacent photographs also occur and these should be dealt with to create a seamless mosaic. These geometric differences are caused by sun-angle-dependent shadows, seasonal reflection changes of fields, forests and water bodies, different atmospheric conditions, and variations in film development procedure (Yehuda & Brand 1998).

The orthorectified NIR and RGB images were mosaicked using the Mosaic tool of ERDAS Imagine Software. Manual colour balancing using the linear surface method

was applied on all the images. The resultant image mosaics were, however, not without problems. Producing a seamless image mosaic without variations in reflectance between overlapping images was not possible. An effort was made to minimise the variations by trying different mosaicking options. Also, geometric mismatches in overlapping images could not be eliminated between some adjacent images. The resultant mosaicked images for both NIR and RGB datasets are shown in Figures 3.3 and 3.4 respectively.

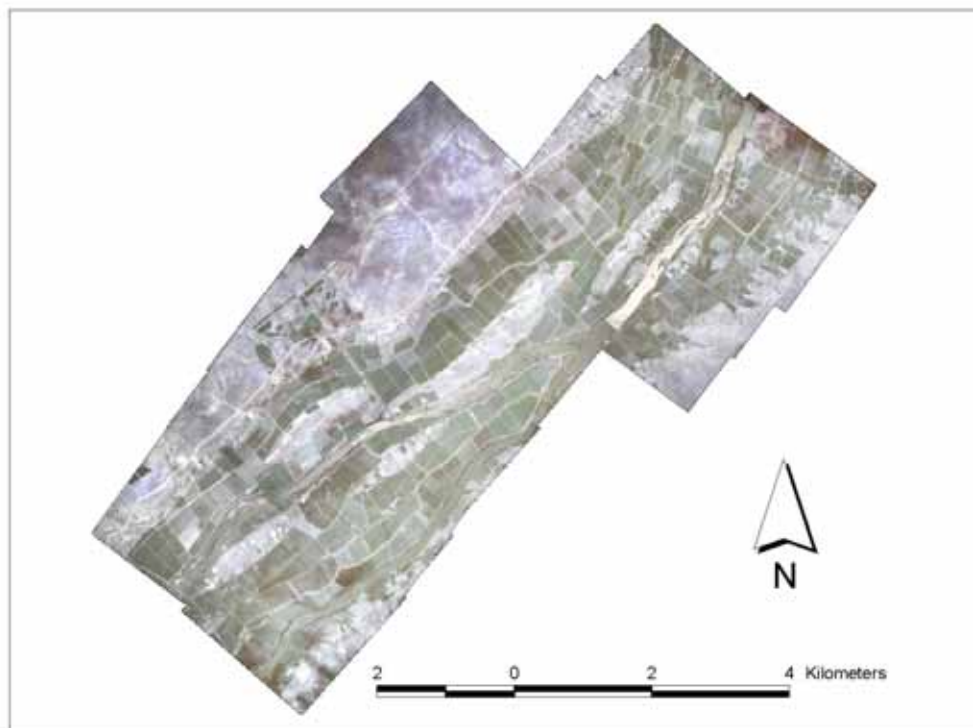


Figure 3.3 Mosaicked RGB images covering the study area

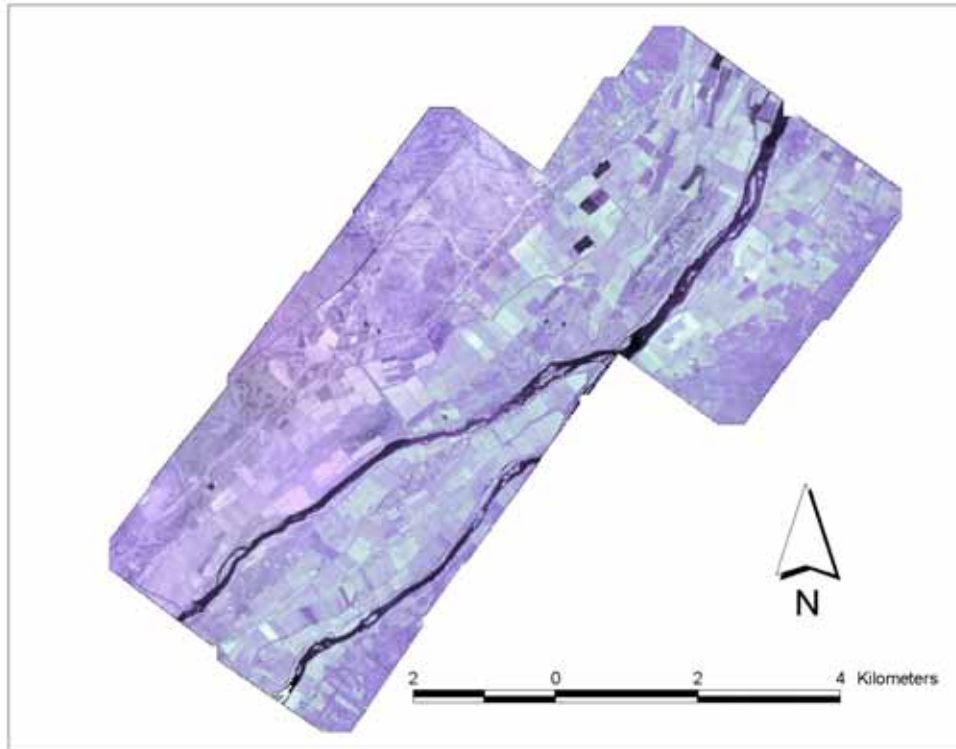


Figure 3.4 Mosaicked NIR images covering the study area

3.4 IMAGE STACKING

The RGB and NIR mosaicked images were stacked to produce one image consisting of four bands. An NDVI image was produced from the resultant stacked image. Bands 4 (NIR band) and 3 (Red band) were used in computing the NDVI values. The stacked image was also used as input in an unsupervised image classification for identification of irrigated and salinised lands in the study area. The NIR and RGB images did not fit precisely on each other when stacked. Areas that were not exactly covered by both images were visible along the outer portions of images. The stacked image displayed with bands 4, 2, and 1 is shown in Figure 3.5.

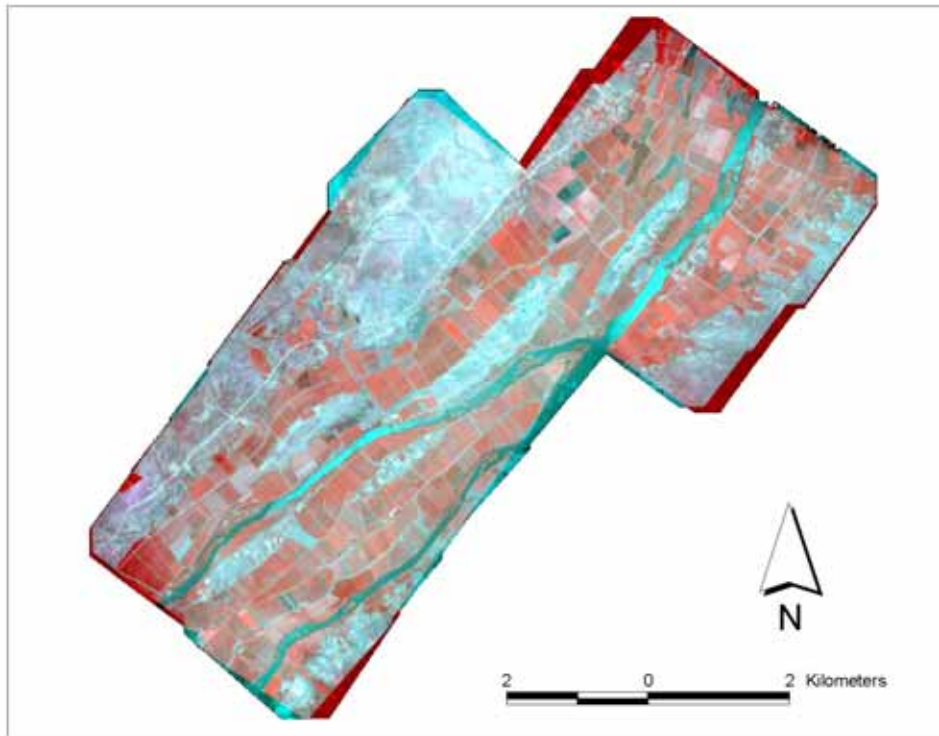


Figure 3.5 Stacked image of the study area

The image analysis techniques carried out on the images are outlined in the following two chapters.

CHAPTER 4: IDENTIFICATION OF CULTIVATED LAND

4.1 INTRODUCTION

Visual air photo interpretation is used in the first part of this chapter to identify cultivated land in the study region. Onscreen digitising was used to delineate cultivated land. In the second part of the chapter, unsupervised image classification was used to identify cultivated land digitally. Lastly, accuracy assessments were employed to determine the success of both methods in identifying cultivated land.

4.2 VISUAL INTERPRETATION

Objects on aerial photographs are distinguished by differences in shapes, tones, texture, and sizes. It is possible to visually identify objects in an aerial photo, thus communicating this information by the use of maps to users. According to Lillesand & Keifer (1979), Campbell (1996), and Sebego & Arnberg (2002), size, shape, pattern, shadow, tone, texture and site are some of the basic characteristics that are useful for visual photo interpretation. For visual image analysis, Lillesand & Keifer (1979) argue that crop classification through photo interpretation is based on the premise that specific crop types can be identified by their spectral response pattern and photo texture. Nevertheless, multi-date photographs may be necessary when similar looking crop types have to be discriminated from one another. However when broad classes of crops have to be inventoried, single-date photographs may be sufficient. Lillesand & Keifer (1979) maintain that the knowledge and experience of the image interpreter is very important in visual image analysis.

Using visual interpretation, the following images were used to identify irrigated land in the study area: mosaicked RGB, NIR mosaicked, stacked (RGB and NIR), and the NDVI images.

4.2.1 Manual classification of the mosaicked RGB image

Manual onscreen digitising was used to digitise cultivated land on the mosaicked RGB image of the study region. Since this exercise was meant to identify cultivated land in the study area, only land used for agriculture was digitised. Agricultural land was divided into two categories, viz. vines and orchards; and other crops and fallow

land. The pattern and texture of the crops were used to isolate vines and orchards from other crop types. As highlighted by Lillesand and Keifer (1979), it proved very difficult to isolate the different categories of vines and other crops. It is because of this difficulty that all categories of vines and orchards were grouped in one class called vines and orchards and a similar grouping of all other crops in a class called other crops and fallow land. Fallow land consisted of land that was not cultivated at the time of the imagery. Because it was very difficult to tell whether some portions of land were covered by grass or planted with some crops (e.g. Lucerne), fallow lands were grouped with crops other than vines and orchards. Cultivated land demarcated from visual interpretation of the mosaicked RGB image is shown in Figure 4.1.



Figure 4.1 Cultivated land demarcated from manual classification of the mosaicked RGB image

4.2.2 Manual classification of the mosaicked NIR image

The same procedure used above was employed to demarcate cultivated land on the NIR mosaicked image. Like the manual classification of mosaicked RGB images, tone, pattern and texture were used to distinguish land cover types from one another. On the NIR image, areas occupied by vegetation appeared in a bright white colour.

Two categories of cultivated land-cover types were identified. Vines and orchards were classified into one class with fallow lands and other crop types in the other. Vines and orchards were distinguished from the other crop types by their tone, pattern, and texture on the image. Other crop types displayed a fine texture while vines and orchards had a coarse texture, with rows of crops distinguishable in other fields. As with the RGB image, it was not possible to distinguish the different types of vines and orchards and those of other crop types. Fallow lands appeared darker and in some cases it was difficult to tell whether they were fallow or planted with crops that were still young. As in the previous manual RGB classification, fallow lands were grouped into the same class with other crop types. Figure 4.2 is the diagrammatic representation of the result of the manual classification of the NIR image.

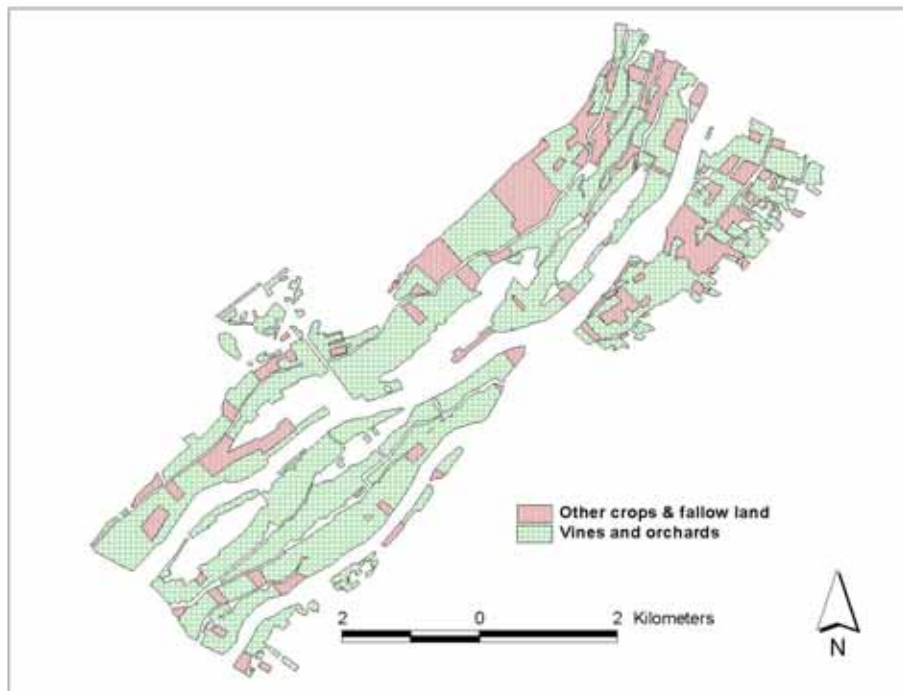


Figure 4.2 Cultivated land demarcated from manual classification of the NIR mosaicked image

4.2.3 Manual classification of the stacked image

As explained in section 3.3 in Chapter 3, the stacked image consists of four bands obtained by stacking the RGB and near infrared bands. Displayed with bands 4, 2 and 1, vegetation appeared bright red on this image. Manual image classification was

conducted by digitising cultivated land. As in the classification of the RGB and NIR images, cultivated land was categorized into two groups: vines and orchards; and, other crops and fallow land. Tone, pattern and texture of the image were used to distinguish vines and orchards, and other crop types. The texture of vines and orchards appeared coarser while that of other crop types was fine. The resultant map obtained from the manual classification of the stacked image is shown in Figure 4.3.



Figure 4.3 Cultivated land demarcated from manual classification of the stacked image

4.2.4 Manual classification of the NDVI image

A normalised difference vegetation index (NDVI) was computed using the stacked image to produce an NDVI image. Manual image classification by the use of onscreen digitising was conducted on the resultant NDVI image. Cultivated land was classified into two classes as was done on the other images. On this image, areas occupied by crops and natural vegetation were clearly distinguishable from the other land cover types as the former appeared bright white on the image. Areas of low NDVI values (non-vegetated areas) appeared darker. On this image, vines and orchards appeared brighter than the other crop types because of their higher NDVI values. Fallow land

and other crop types had lower NDVI values compared to vines and orchards and appeared less bright on the image. Non-vegetated areas appeared darker on this image. Distinguishing fallow lands and fields where crops were still young proved difficult on the NDVI image. Cultivated land obtained from manual classification of the NDVI image is shown in Figure 4.4.

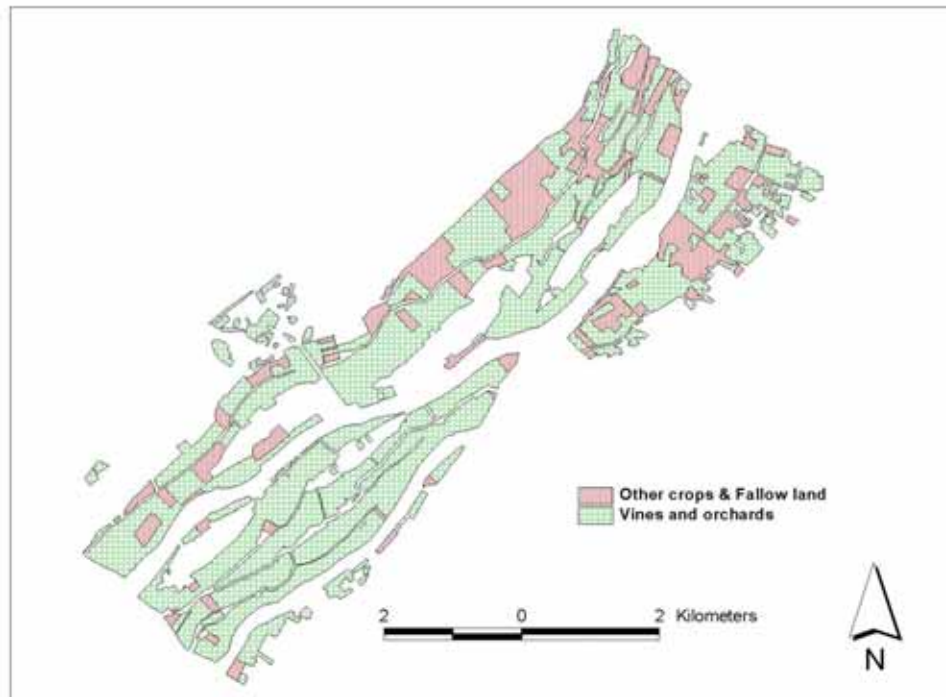


Figure 4.4 Cultivated land demarcated from manual classification of the NDVI image

4.3 DIGITAL IMAGE ANALYSIS

Digital image classification is one of the techniques used for feature extraction in digital image analysis. Several classification methods are available for classification of remotely sensed data as outlined in section 2.3.3.1. The literature studied did not indicate which of the methods are the best in classifying remote sensing data, but it showed that each method has its own advantages and disadvantages. According to Lillesand & Keifer (1979), using a combination of these classification methods produces better results. Unsupervised image classification is the technique used in this study.

As outlined in ERDAS (2002), ISODATA which is the only available algorithm for unsupervised image classification in the package, uses minimum spectral distance to assign pixels to a cluster. This process begins with a specified number of arbitrary cluster mean(s) of the existing signatures and then it processes repetitively, so that those means shift to the means of the clusters in the data. Because the ISODATA is iterative, it is not biased to the top of the data file like the one-pass clustering algorithms. Performing an ISODATA clustering requires a specification of the number of clusters, convergence threshold, and the maximum number of iterations to be performed.

Unsupervised classification was conducted on each of the four datasets, viz. RGB mosaicked, NIR mosaicked, stacked, and the NDVI images to isolate cultivated land in the study area. The NIR mosaicked image was not very successful in separating land-cover types, e.g. vines and orchards from other crop types, and fallow from barren lands. Unsupervised classification of this image was not pursued further for analysis of cultivated land. Thus, unsupervised classification of the RGB mosaicked, stacked, and NDVI images were investigated further for the identification of cultivated land.

Classifying the images into many classes produced images that were difficult to interpret. A fifteen-class classification for all the images produced results that were interpretable. Three broad land-cover categories were isolated from the classified images, viz. vines and orchards, other crops and fallow lands, and other land cover types. The category of other land cover types consists of pixels covering water, built-up areas, barren lands, and all other land cover types not related to irrigated land merged together. The classification of each of the RGB mosaicked, stacked, and the NDVI images are presented in the subsections that follow.

4.3.1 Unsupervised classification of the RGB mosaicked image

According to Campbell (2002) and Lillesand & Keifer (1979), the most difficult part of unsupervised classification is assigning information classes to spectral classes. Using the RGB mosaicked image as a reference, spectral classes were assigned to information classes. Unsupervised classification produced a number of subclasses that needed to be combined in order to generate classes that correspond with those

generated by visual image classification technique. Portions of forests, trees and shrubs were included in one category as vines and orchards. Crops other than vines and orchards also could not be identified as single classes. Pixels covering areas occupied by grass, weeds, etc. were included in this category. Similar classes were grouped to produce single classes. Figure 4.6 shows cultivated land derived from an unsupervised classification of the RGB mosaicked image.

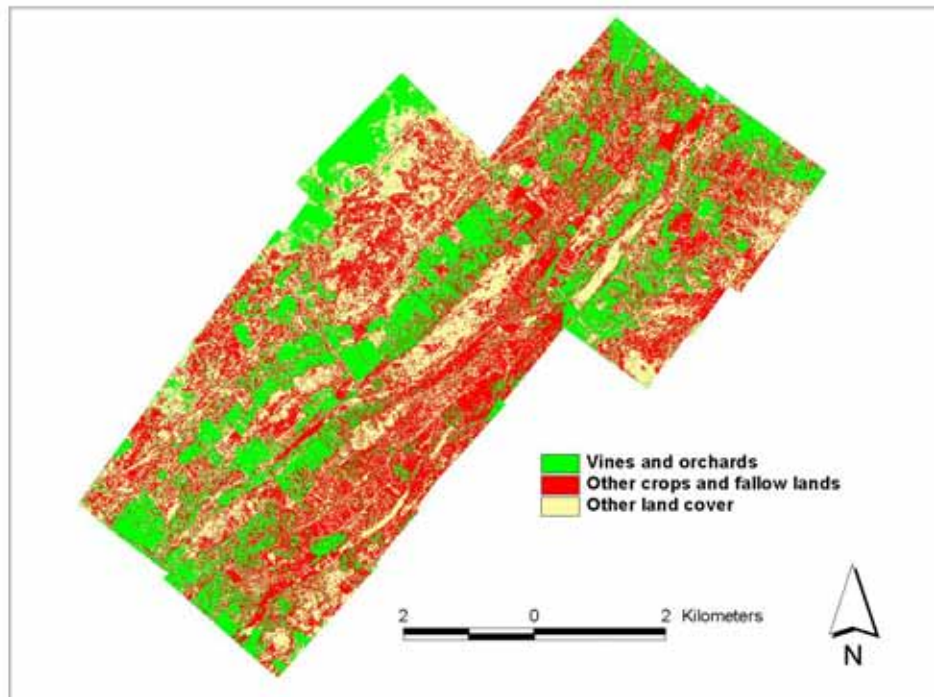


Figure 4.5 Cultivated land demarcated from unsupervised classification of the mosaicked RGB image

It is evident from Figure 4.6 that there were difficulties in separating fallow lands and barren areas. There are many pixels outside the cultivated area that are visible on the map, which fall into the category of other crops and fallow land. This is probably the result of the difficulty of the classifier to separate fallow lands, barren areas, grass, etc.

4.3.2 Unsupervised classification of the stacked image

As in the RGB mosaicked image classification above, the RGB mosaicked image was used as the basic information in assigning spectral classes to information classes. As in the RGB mosaicked image classification, subclasses produced by unsupervised

classification needed to be combined to generate classes that correspond to those generated by visual image interpretation technique. Three broad land-cover types were identified, viz. vines and orchards, other crops and fallow lands, and other land cover. Cultivated land obtained from unsupervised classification of the stacked image is depicted in Figure 4.8.

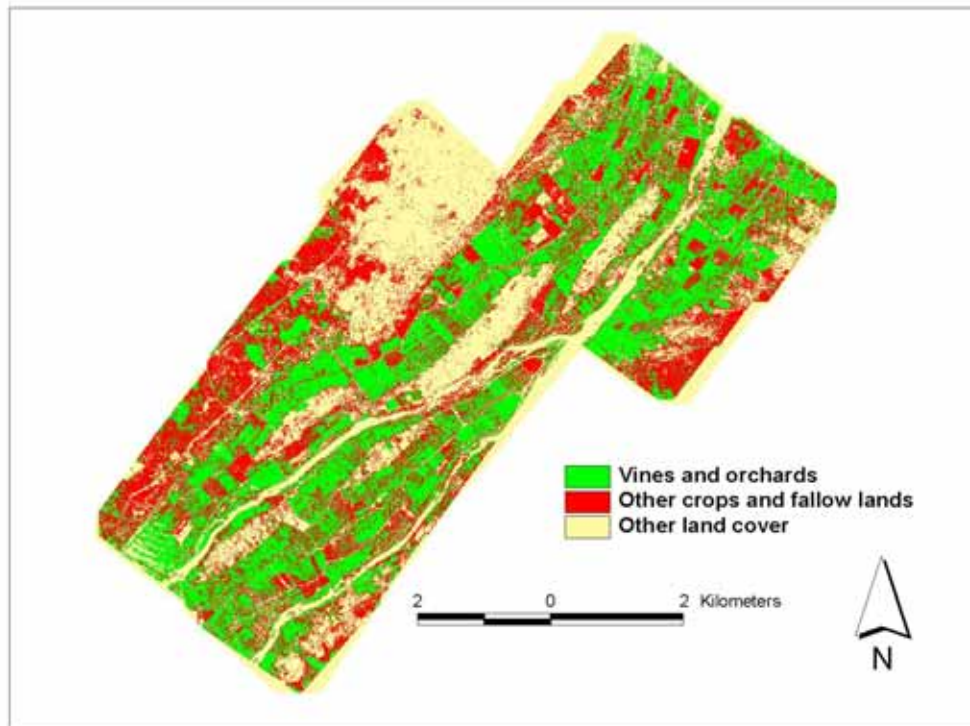


Figure 4.6 Cultivated land demarcated from unsupervised classification of the stacked image

Unsupervised classification of the stacked image also shows difficulties in separating some land-cover types from one another. However, the extent of those overlapping classes is not severe as in the classification of the RGB mosaicked image.

4.3.3 Unsupervised classification of the NDVI image

As in all the above images, the NDVI image was classified into fifteen classes. Classes identifying vines and orchards, other crops and fallow lands, and other land cover types were identified using the RGB mosaicked image as the basic information. Unsupervised classification of the NDVI image also revealed difficulties in separating land cover types. Cultivated land demarcated from unsupervised classification of the NDVI image is depicted in Figure 4.7.

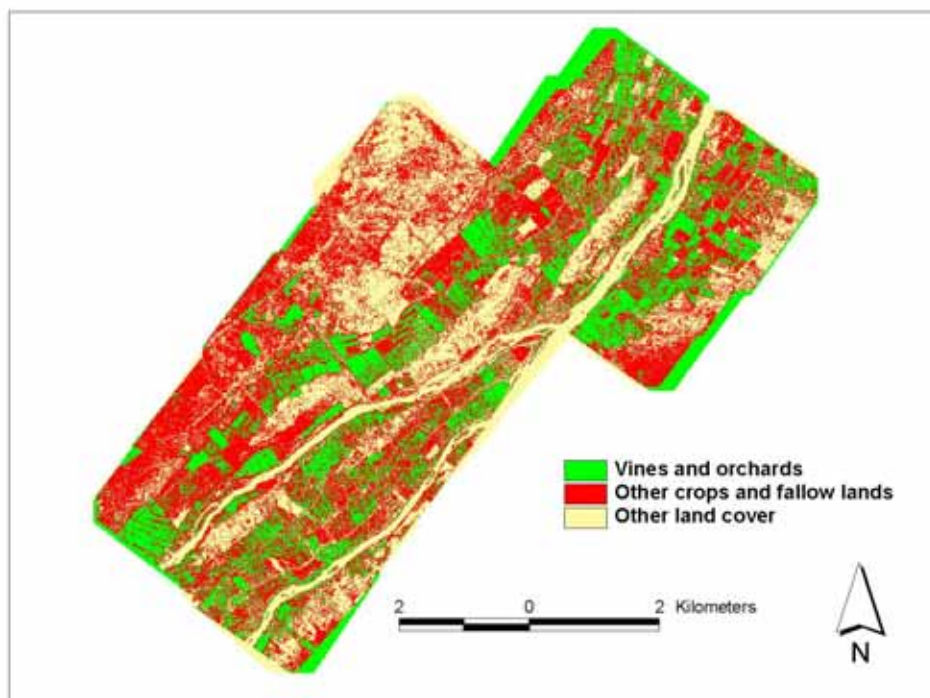


Figure 4.7 Cultivated land demarcated from unsupervised classification of the NDVI image

To determine the degree of success for both the manual and digital classification methods in the identification of cultivated land, accuracy assessments were conducted. The accuracy assessments of all the classified images are evaluated and expounded in the section that follows.

4.4 ACCURACY ASSESSMENT

Land-cover types on sampled sites were identified when the samples were collected. These data on land-cover types was used to conduct classification accuracy of both the manual and digital classification methods. Confusion matrices were constructed after the field reference data was overlaid with the classified images. In these tables, errors of commission and omission are tabulated, and the percentage land cover correctly classified is calculated by dividing the sum of the diagonals by the total. In the confusion matrices, producers' accuracy (PA) refers to the probability of a land use category on the ground being correctly identified on the map (Lenney et al. 1996). PA is the ratio of the cell probability of the correctly identified sites to the true proportion of that class on the ground. Consumer's accuracy (CA) is a guide to the

reliability of a map as a predictive device and gives the user of the map the percentage of each land cover category that is identified accurately by the prediction technique (Campbell 2002).

The accuracy assessments of each of the classification techniques are presented in the subsections that follow.

4.4.1 Manual image classification

In order to be as accurate as possible, an area within 3m of the sampled point was assumed to be representative of the land cover type of the sampled point. Buffer zones of 3m were computed around sampled points (see Figure 4.8 for points around which buffer zones were created). Both the buffer shape files and the classified images were converted to grids of cell size 0,75m. A combinatorial-AND operation in the GRID module of ARCInfo software was used to compare each set of the classified data with the reference grid (gridded ground truth data). This operation compares two grids on a cell-by-cell basis and produces a grid that gives the number of cells for each combination. In this way, all the correctly classified and the incorrectly classified cells are shown. The data from the resultant grids were used to compute confusion matrices for each classified image. The statistics of these errors for all the images are tabulated in Tables 4.1 to 4.4.

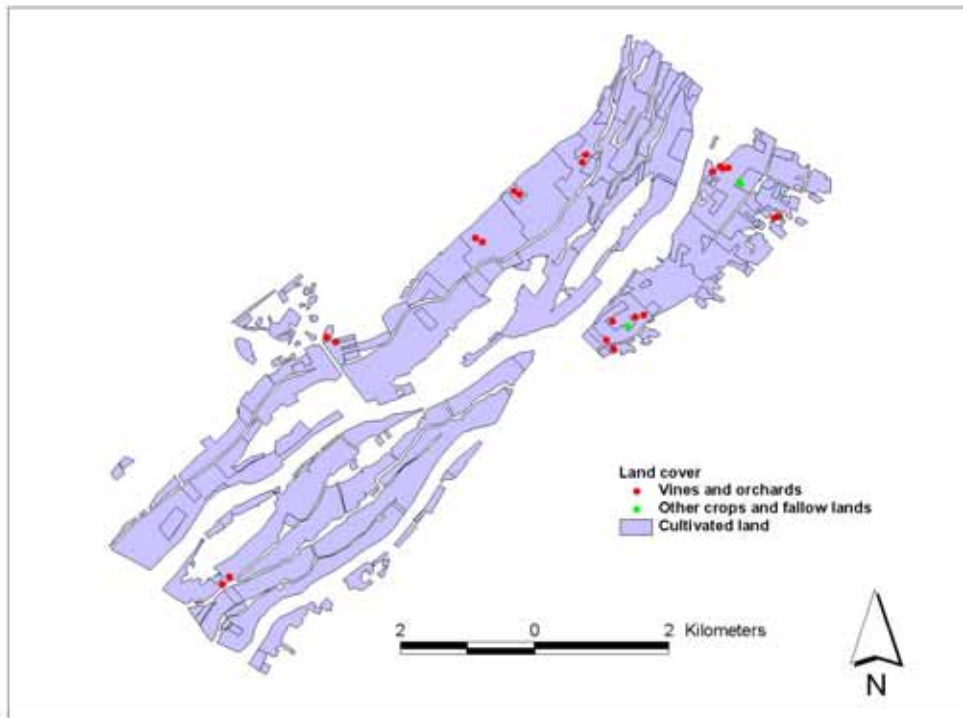


Figure 4.8 Land use at field sample points

Table 4.1 Confusion matrix comparing cultivated land identified by manual classification of the RGB mosaicked image with ground truth data

RGB manually classified image	Ground truth			
	Vines and orchards	Other crops and fallow land	Total	CA%
Vines and orchards	992	0	992	100
Other crops and fallow land	57	149	206	72,3
Total	1049	149	1198	
PA%	94,6	100		

Percentage correct 95,2

Table 4.2 Confusion matrix comparing cultivated land identified by manual classification of the NIR image with ground truth data

NIR manually classified image	Ground truth			
	Vines and orchards	Other crops and fallow land	Total	CA%
Vines and orchards	1001	0	1001	100
Other crops and fallow land	48	149	197	75,6
Total	1049	149	1198	
PA%	94,7	100		

Percentage correct 95,9

Table 4.3 Confusion matrix comparing cultivated land identified by manual classification of the stacked image with ground truth data

Stacked manually classified image	Ground truth			
	Vines and orchards	Other crops and fallow land	Total	CA%
Vines and orchards	994	0	994	100
Other crops and fallow land	55	149	204	75,6
Total	1049	149	1198	
PA%	95,4	100		

Percentage correct 95,4

Table 4.4 Confusion matrix comparing cultivated land identified by manual classification of the NDVI image with ground truth data

NDVI manually classified image	Ground truth			
	Vines and orchards	Other crops and fallow land	Total	CA%
Vines and orchards	899	0	899	100
Other crops and fallow land	150	149	299	49,8
Total	1049	149	1198	
PA%	85,7	100		

Percentage correct 87,5

The statistics in Tables 4.1 to 4.4 show that manual classification of the images for the identification of irrigated land was a success. All the images except the manual classification of the NDVI images achieved accuracies greater than 95% (refer to Tables 4.1 to 4.4). The average percentage of correctly classified land cover by the four images is 93,5% with the average probability of vines and orchards being correctly classified by all the images at 92,6% while that of other crops and fallow lands is 100%. Manual classification was able to identify most of the vines and orchards as indicated by higher CA percentages in all the tables above. On average only 61,4% of other crops and fallow lands were identified correctly by the different techniques. While the statistics in the tables above indicate the high degree of success of manual classification of the four images, it should be acknowledged that this has been achieved due to the broad classes delimited.

Accuracy assessments for identification of cultivated land by using unsupervised image classification are presented in the following section.

4.4.2 Digital image classification

As with the accuracy assessment of the manually classified images, the statistics of errors of commission and omission for digital image classification were obtained from the comparison of the grids of ground truth data and the classified images. Statistics for errors of commission and omission for each classified image are depicted in Tables 4.6 to 4.8. Because the reference grid only had two classes while the grids obtained from the classification of the images had three classes, there were no pixels tabulated for other land cover types (see Tables 4.5 to 4.7).

Table 4.5 Confusion matrix comparing cultivated land identified by unsupervised classification of the RGB mosaicked image with ground truth data

Classified RGB image	Ground truth				
	Vines and orchards	Other crops and fallow land	Other land cover	Total	CA%
Vines and orchards	387	1	0	388	99,7
Other crops and fallow land	345	100	0	445	22,5
Other land cover	317	48	0	365	0
Total	1049	149	0	1198	
PA%	36,9	67,1	0		

Percentage correct 40,7

Table 4.6 Confusion matrix comparing cultivated land identified by unsupervised classification of the stacked image with ground truth data

Classified stacked image	Ground truth				
	Vines and orchards	Other crops and fallow land	Other land cover	Total	CA%
Vines and orchards	721	11	0	732	98,5
Other crops and fallow land	241	96	0	337	28,5
Other land cover	87	42	0	129	0
Total	1049	149	0	1198	
PA%	68,7	64,4	0		

Percentage correct 68,2

Table 4.7 Confusion matrix comparing cultivated land identified by unsupervised classification of the NDVI image with ground truth data

Classified NDVI image	Ground truth				
	Vines and orchards	Other crops and fallow land	Other land cover	Total	CA%
Vines and orchards	542	7	0	549	98,7
Other crops and fallow land	444	127	0	571	22,2
Other land cover	57	15	0	72	0
Total	1043	149	0	1192	
PA%	51,9	85,2	0		

Percentage correct 56,1

Judging from the statistics in Tables 4.5 to 4.7, unsupervised classification for the identification of cultivated land was not as successful as the manual classification. With the percentage of correctly classified land cover at 68,2%, the stacked image performed better than the RGB mosaicked and the NDVI images, which attained 40,7% and 56,1% respectively. All the images managed to correctly classify most of the vines and orchards and failed to classify most of other crops and fallow land as shown by higher CA percentages for vines and orchards while those of other crops and fallow land are lower (refer to Tables 4.5 to 4.7). A significant percentage of vines and orchards were incorrectly classified as other crops and fallow land on all the images (32,9%, 23% and 42,6% for RGB, stacked and NDVI images respectively). Thus, unsupervised classification of these images shows difficulties in separating certain land cover types, e.g. vines and orchards from other crops and fallow land.

Digital image analysis revealed difficulties in identifying cultivated land in the study area as shown by lower percentages of correctly identified land cover. This is partly due to the inability of the classifier to separate land cover types based on single-date imagery. Also, the images were not radiometrically calibrated because of lack of camera model information. Similar objects may show different reflectance properties due to the differences in times of the day that the imagery were captured.

Manual classification of the RGB mosaicked, NIR mosaicked, and the stacked images attained the highest accuracies in the identification of cultivated land. These images

were used to calculate the extent of cultivated land in the study area. The area was calculated by multiplying the number of pixels of each category of cultivated land on each image by the area of a pixel. The resultant area for each category was corrected using the percentage accurate (PA) for each of the vines and orchards, and other crops and fallow lands as a correction factor. The calculated areas for both vines and orchards and other crops and fallow lands were added for the three images involved. The average area occupied by vines and orchards, and other crops and fallow land is 1609 and 515 hectares respectively. The total surface area of cultivated land in the study area is thus 2124 hectares.

Identification of potentially salinised lands is presented in the following chapter.

CHAPTER 5: IDENTIFICATION OF SALINISED LAND

5.1 INTRODUCTION

The two techniques, viz. visual and digital air photo interpretation, used in the previous chapter to identify irrigated land are again employed in this chapter to identify potentially salinised land. The NIR, and the NDVI images were used to identify potentially salinised land visually. Again, because of the failure of the NIR in separating land-cover types by unsupervised classification, only RGB mosaicked, stacked, and NDVI images were used to identify salinised land. The first part of the chapter deals with the visual air photo interpretation and is then followed by the digital image analysis. Results of soil samples collected and analysed for salinity are integrated in the last part of the chapter to validate the results of the visual and digital image analysis techniques in identifying salinised land.

5.2 AIR PHOTO INTERPRETATION

Interpretation of aerial photographs can be used in assessing crop diseases, insect damage, plant stress and damage due to disaster. According to Lillesand and Keifer (1979), aerial photo interpretation for crop condition assessment is much more difficult than airphoto interpretation for crop type and area inventory. Lillesand and Keifer (1979) argue that it is difficult to distinguish the effects of diseases, insect damage, nutrient deficiencies or drought from variations caused by plant variety, plant maturity, planting rate or background soil differences.

Studies by Penuelas et al. (1997) and Wang, Wilson and Shannon (2002) found that saline conditions decrease near infrared reflectance while increasing visible reflectance. According to Campbell (2002), the spectral characteristics of a plant leaf may change as a result of stress by disease, insect attack, or moisture shortage. Campbell (2002) further argues that although these changes occur more or less simultaneously in both the visible and the near infrared regions of the electromagnetic spectrum, changes in the near infrared region are more noticeable. On NDVI images displayed in grey scale, vegetated areas appear brighter than non-vegetated areas because of their higher NDVI values. Also, areas of stressed vegetation on different fields will be distinguished by appearing darker because of lower NDVI values. Thus,

potentially salinised areas will be relatively easier to identify on the NIR, and the NDVI images. Therefore, the NIR mosaicked, and the NDVI images were used in the identification of potentially salinised land visually.

The use of each of these images in identifying salinised land is discussed in the following subsections.

5.2.1 Visual analysis of the NIR mosaicked image

Although near infrared bands are said to identify stressed vegetation better than the visible bands, identifying potentially salinised land on these images was not simple. Healthy vegetation on NIR images appeared as a bright white colour. Areas where vegetation was stressed appeared darker on the images. Difficulties were experienced in identifying potentially salinised land where crops were still young. On these areas, more soil was exposed, making it difficult to identify areas where vegetation showed stress. Figure 5.1 shows potentially salinised land obtained by visual analysis of the NIR images.

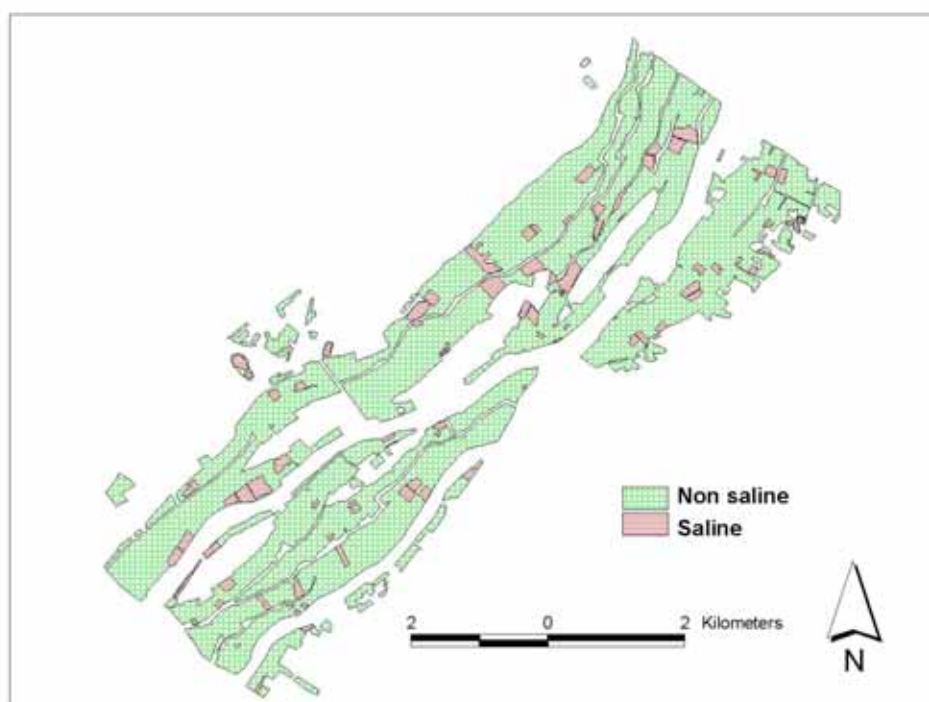


Figure 5.1 Salinised land identified by visual interpretation of the NIR mosaicked image

Out of the 2124 hectares of cultivated land in the study area, 179,4 hectares of irrigated land was identified as salinised by visual analysis of the NIR mosaicked image. This constitutes 8.4% of cultivated land in the study region.

5.2.2 Visual analysis of the NDVI image

On the NDVI image displayed on a grey scale, healthy vegetation appeared white and areas of low NDVI values appeared dark. Potentially salinised lands on this image were relatively easier to locate. These areas appeared darker compared to areas occupied by healthy vegetation. As on the NIR mosaicked image, it was difficult to identify potentially salinised areas where crops were still young. These areas exposed more soil than vegetation, making these areas look darker. Potentially salinised areas on this image were digitised onscreen and represented in Figure 5.2.

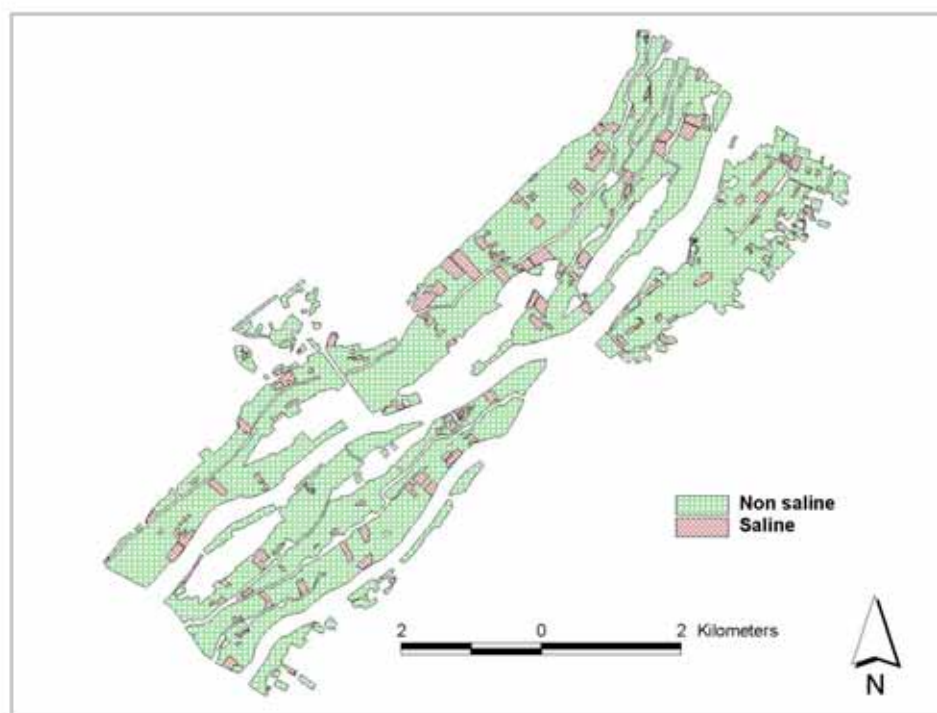


Figure 5.2 Salinised land identified by visual interpretation of the NDVI image

Visual analysis of the NDVI image revealed that 208,9 hectares (9.8%) of cultivated land in the study area is affected by salinisation.

Unsupervised classification is used in the following section to identify potentially salinised land digitally.

5.3 DIGITAL IMAGE ANALYSIS

In this section, unsupervised image classification is employed to isolate potentially salinised land. RGB mosaicked, stacked, and the NDVI images were subjected to an unsupervised image classification technique. The resultant classified images are analysed for potentially salinised land. Because unsupervised image classification identifies natural groupings in the data, it is hoped that potentially salinised lands will be identified in these groupings. Also, since fields are supposed to be cultivated with crops of the same type and age, deviations in reflection of electromagnetic radiation should be revealed when the images are classified. Classes of salinised areas will appear as patchy areas on cultivated fields.

An unsupervised classification of each of the images for identification of salinised land is presented in the following subsections.

5.3.1 Unsupervised classification of the RGB mosaicked image

After the RGB mosaicked image was classified into fifteen classes, the classified image was analysed with the NDVI image as the basic information. Because of their lower NDVI values, pixels covering potentially salinised areas appeared darker on the NDVI image. These areas appeared as patchy areas on fields on the classified image. Unsupervised classification was unable to identify these areas as single classes. These potentially salinised areas also covered fallow land, bare soil, grasses and bushes, and barren land on some portions of the classified image.

Pixels covering areas of healthy crops were grouped to produce one class called non-saline land. The same procedure was used to combine all classes covering potentially salinised land and those of other land-cover types. The amount of land identified as salinised by this image is 1042,8 hectares (about 49%). Figure 5.3 shows potentially salinised land obtained from unsupervised classification of the RGB mosaicked image.

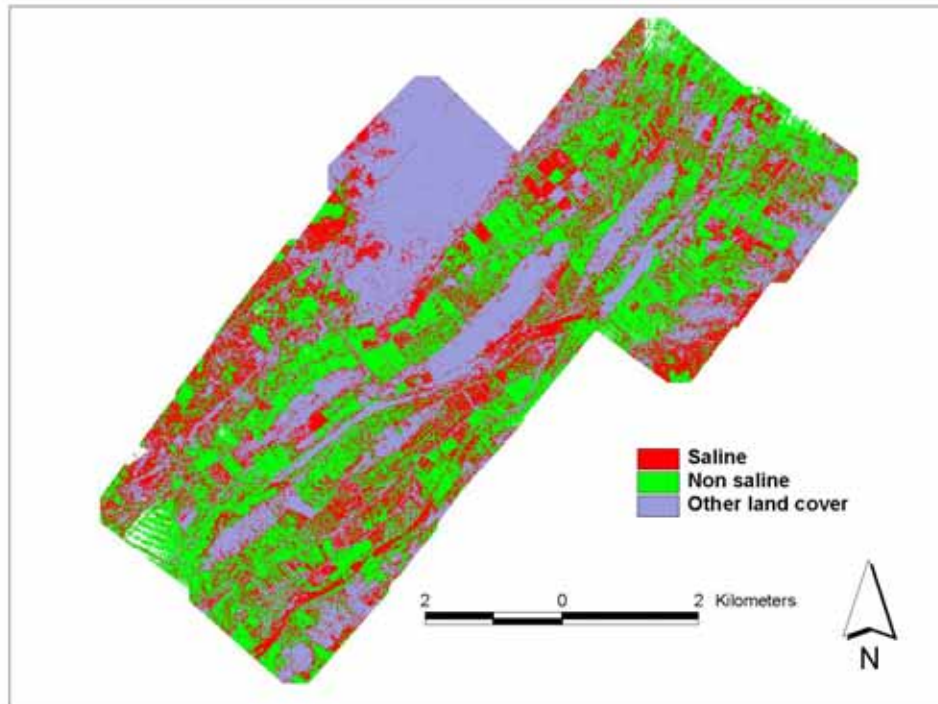


Figure 5.3 Salinised land identified by unsupervised classification of the RGB mosaicked images

5.3.2 Unsupervised classification of the stacked image

Again, using the NDVI image the basic information classes identifying potentially salinised areas were identified on the classified stacked image. As in the unsupervised classification of the RGB mosaicked image, unsupervised classification of the stacked image was also unable to identify potentially salinised areas in single classes. Other vegetation types that are not necessarily stressed were classified with potentially salinised crops. These vegetation groups may have similar reflectance values to potentially salinised vegetation. Pixels identifying salinised land were merged together. The same procedure was applied to merge pixels of non-salinised land, and also those of land-cover types other than irrigated crops. This image predicted that 1245,2 hectares (about 59%) are salinised. Salinised land obtained from unsupervised classification of the stacked image is depicted in Figure 5.4.

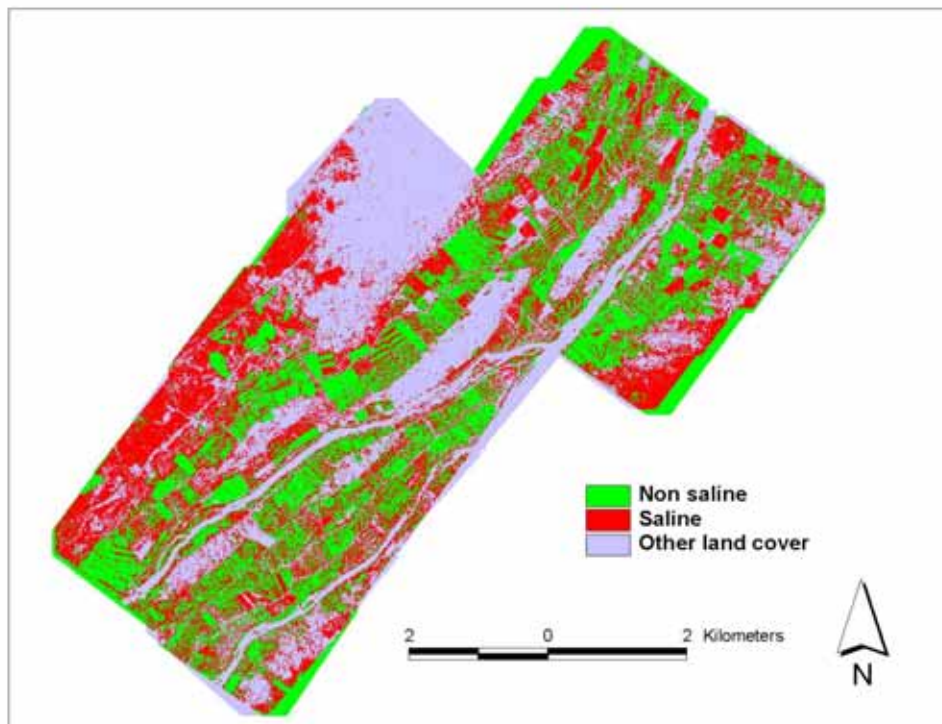


Figure 5.4 Salinised land identified by unsupervised classification of the stacked image

Unsupervised classification of the stacked image also classified potentially salinised areas with other land-cover types, which may not necessarily be salinised. These pixels are visible on areas outside irrigated areas. These areas may not necessarily be salinised, but vegetation identified in these pixels may be showing similar reflectance patterns to crops affected by salinisation.

5.3.3 Unsupervised classification of the NDVI image

Like the other images, the NDVI image was subjected to unsupervised image classification into fifteen classes. The classified image was compared with the NDVI image in order to identify potentially salinised land. As in the other two images above, pixels covering potentially salinised land were merged. A similar procedure used in the two sections above was applied to combine pixels of non-salinised land, and those of land-cover types other than vegetation. Potentially salinised land obtained from unsupervised classification of the NDVI image amounts to 1053,6 hectares (about 50%). Salinised land obtained from unsupervised classification of the NDVI image is depicted in Figure 5.5.

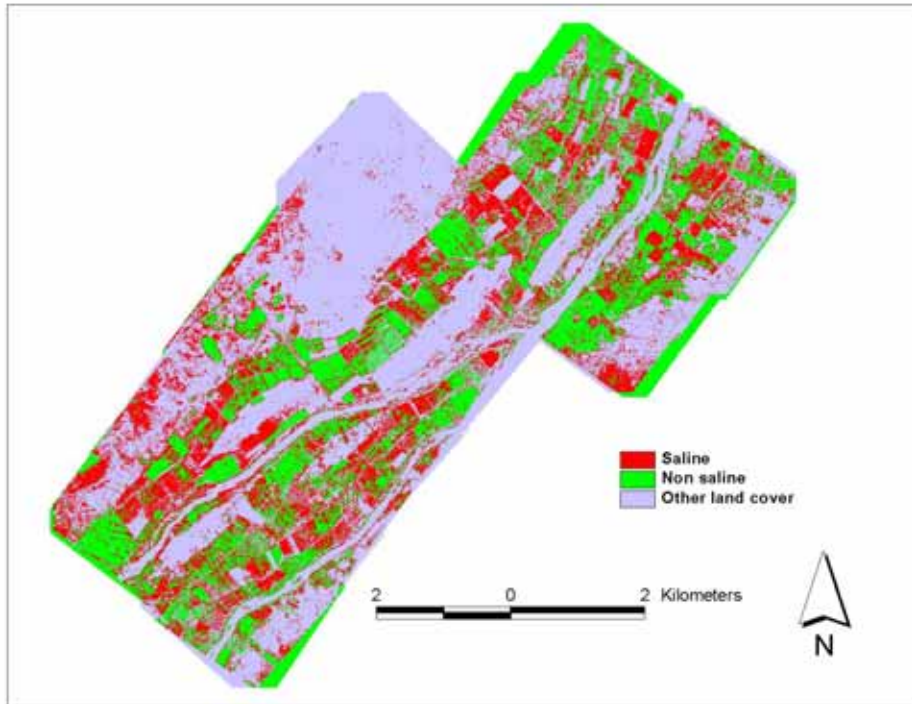


Figure 5.5 Salinised land obtained from unsupervised classification of the NDVI image

Pixels identifying potentially salinised areas were classified with other pixels located outside areas of irrigated land. These areas may not necessarily be salinised, but they may be occupied by vegetation that has similar reflectance patterns to salinised crops.

5.4 FIELD VALIDATION

Soil samples collected from 12 randomly selected potentially salinised plots taken for the larger WRC survey which were analysed for salinity, and another 12 from potentially non-salinised plots in the same survey were extracted for this study area. These paired samples were used to validate the results of salinised land obtained by visual and digital image analysis techniques. This validation is explained in the following subsections.

5.4.1 Visual image analysis

In order to make the validation as accurate as possible, an area within 3m of each sampled point was assumed to be representative of the results of that point. Buffer zones of 3m were created around sampled points (see Figure 5.6 for points around

which buffer zones were created). A value grid of cell size 0,75m indicating salinised and non-salinised areas was created from the buffer shapefiles. This grid was overlaid on the grids of potentially salinised land obtained from visual analysis of each of the NIR, and the NDVI images. Using the results obtained from each overlay, confusion matrices (Tables 5.1 and 5.2) were constructed to validate the results.

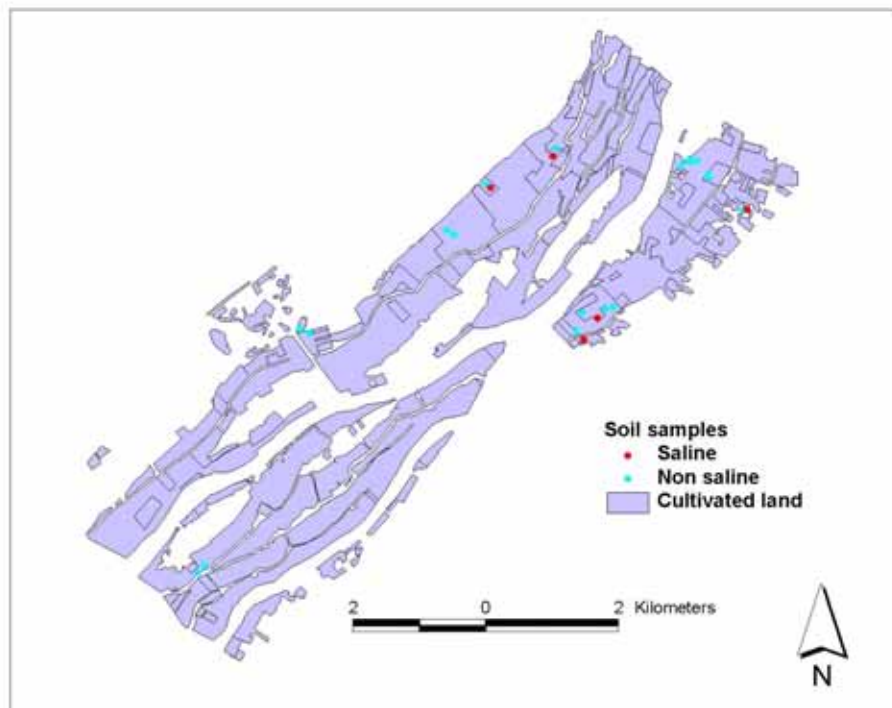


Figure 5.6 Salinity at field sample points

Table 5.1 Confusion matrix comparing potentially salinised land identified by visual analysis of the NIR mosaicked image with analyzed soil samples

NIR salinised land	Field samples			
	Actual saline	Actual non-saline	Total	CA%
Potential saline	151	155	306	49,3
Potential non-saline	250	650	900	72,2
Total	401	805	1206	-
Percentage	33,3	66,7	100	-
PA%	37,7	80,7	-	-

Percentage correct 66,4%

Table 5.2 Confusion matrix comparing potentially salinised land identified by visual analysis of the NDVI image with analyzed soil samples

NDVI salinised land	Field samples			
	Actual saline	Actual non-saline	Total	CA%
Potential saline	186	120	306	60,8
Potential non-saline	247	653	900	72,5
Total	433	773	1206	-
Percentage	35,9	64,1	100	-
PA%	42,9	84,5	-	-

Percentage correct 69,6%

From the statistics in the Tables 5.1 and 5.2 above, visual analysis of the NIR mosaicked and NDVI images respectively achieved 66,4% and 69,6% accuracy in identifying salinised and non-salinised land in the study area. Analysis of field samples indicate that visual analysis of the NIR mosaicked image could only correctly identify 49,3% of salinised land (see Table 5.1). The probability of salinised land being correctly identified by visual analysis of the NIR image is low at 37,7%. Visual analysis of the NIR mosaicked image correctly identified most of non-salinised land (72,2%).

Visual analysis of the NDVI image managed to correctly identify more salinised land than visual analysis of the NIR mosaicked image. About 61% of salinised land was correctly identified by visual analysis on this image. Although still low, the

probability of salinised land being correctly identified by visual analysis on this image is higher than on visual analysis of the NIR image (see PA in Table 5.1 and 5.2). This image too managed to identify most of non-salinised land (72.2%).

Although not entirely satisfactory, a fair amount of salinised land was identified by visual analysis of the NIR mosaicked, and the NDVI images. As the statistics in Tables 5.1 and 5.2 suggest, the NDVI image performed better than the NIR mosaicked image in identifying salinised land. The failure of the images to identify more salinised land is probably due to an inability to differentiate stress caused by salts from other forms of stress. Potentially salinised areas on these two images were identified by virtue of vegetation revealing deviations in reflecting electromagnetic radiation. Other forms of stress, e.g. waterlogging, diseases, sandy soils, etc. could be responsible for differences in reflection values.

Validation of potentially salinised land obtained by digital analysis is presented in the following section.

5.4.2 Digital image analysis

Each of the images classified and analysed for potentially salinised land was converted to grids of cell size 0.75m. All grids were clipped, using a coverage that was digitised to cover irrigated land in the study area. This was done to minimise the effects of pixels outside the irrigated part of the study area.

An area within 3m of each sampled point was assumed to be representative of the results of that point. Thus, a 3m buffer was constructed around all the sampled points (see Figure 5.6 for points around which buffer zones were created). A value grid (cell size 0,75m) representing potentially saline and non-saline areas was computed from the buffers. Using the combinatorial-AND operation in GRID, this grid was compared with each of the grids of potentially salinised land obtained from unsupervised classification of each of the RGB mosaicked, NDVI, and stacked images. Confusion matrices presented in Tables 5.3, 5.4, and 5.5 were constructed from the results obtained.

Table 5.3 Confusion matrix comparing potentially salinised land identified by unsupervised classification of the RGB image with analyzed soil samples

RGB salinised land	Field samples				
	Actual saline	Actual non-saline	Other land cover	Total	CA%
Potential saline	81	280	0	361	22,4
Potential non-saline	140	495	0	635	77,9
Other land cover	72	114	0	186	0
Total	293	889	0	1182	-
Percentage	24,8	75,2	0	100	-
PA%	27,6	55,7	0	-	-

Percentage correct 48,7

Table 5.4 Confusion matrix comparing potentially salinised land identified by unsupervised classification of the stacked image with analyzed soil samples

Stack salinised land	Field samples				
	Actual saline	Actual non-saline	Other land cover	Total	CA%
Potential saline	92	280	0	372	24,7
Potential non-saline	148	520	0	668	77,8
Other land cover	66	100	0	166	0
Total	306	900	0	1206	-
Percentage	25,4	74,6	0	100	-
PA%	30,1	75,8	0	-	-

Percentage correct 50,7

Table 5.5 Confusion matrix comparing potentially salinised land identified by unsupervised classification of the NDVI image with analyzed soil samples

NDVI salinised land	Field samples				
	Actual saline	Actual non-saline	Other land cover	Total	CA%
Potential saline	129	318	0	447	28,9
Potential non-saline	111	477	0	588	81,1
Other land cover	66	105	0	171	0
Total	306	900	0	1206	-
Percentage	25,4	74,6	0	100	-
PA%	42,2	53	0	-	-

Percentage correct 50,3

Unsupervised classification of the RGB mosaicked, stacked, and NDVI images respectively achieved 48,7%, 50,7%, and 50,3% accuracies in identifying salinised and non-salinised land. The amount of salinised land correctly identified by unsupervised classification of the three images is far less than that correctly identified by visual analysis of the NIR, and the NDVI images as shown by the CA percentages (see Tables 5.1 to 5.5). Unsupervised classification of the NDVI image correctly identified more salinised land (28,9%) than the RGB mosaicked, and the stacked images which identified 22,4% and 24,7% respectively. The probability of salinised land being correctly classified by unsupervised classification of the RGB mosaicked, stacked, and the NDVI images is low (27,6%, 30,1%, and 42,2% for the RGB mosaicked, stacked, and NDVI images respectively).

The statistics in Tables 5.3 to 5.5 suggest that unsupervised classification of the three images involved had difficulties in identifying salinised land. On average 66,7% of saline pixels in the field samples were incorrectly identified as non-saline. Thus, unsupervised classification of these images had difficulties in separating salinised crops from other land-cover types which have similar reflectance properties. Inability to differentiate the salt induced stress from other forms of stress when using unsupervised classification also contributed to the poor results.

The overall findings of the study, and the recommendations and directions for further study are presented in Chapter 6.

CHAPTER 6: SYNTHESIS

6.1 INTRODUCTION

This chapter presents the overall findings of the study by evaluating the objectives of the study. Evaluation of the objectives is dealt with in the first part of the chapter. Recommendations and directions for further study are presented in the second part of this chapter. This section concludes the chapter and the study.

6.2 FINDINGS OF THE STUDY

As stated in section 1.4, the overall aim of this study was to evaluate the potential of digital aerial imagery in identifying salinised cultivated land in the selected study area. The three objectives set to realise this aim are presented in section 1.4. Two techniques, viz. visual, and digital image analysis were employed to realise this goal.

The statistics in the confusion matrices in Tables 4.1 to 4.4 show that identification of cultivated land by visual classification of the RGB mosaicked, NIR mosaicked, stacked, and the NDVI images was fairly successful. On the other hand, unsupervised classification was not successful in isolating cultivated land. The percentage of land cover correctly classified is low. This is possibly the result of the classifier failing to differentiate certain land-cover types. Also, only single-date images were used to conduct the study. It is very difficult for a statistical classification algorithm to separate certain land-cover types using single-date images, such as for example fallow lands from barren lands.

Although visual image analysis could not differentiate salt-induced stress from other forms of stress, a fair amount of salinised cultivated land was identified by this technique. Visual analysis of the NDVI image proved more useful in identifying stressed crops. Visual analysis of this image managed to identify about 61% of salinised crops. Visual image analysis of digital aerial images can only be useful in surveying crops affected by stress but not to identify a particular kind of stress.

Digital image analysis by means of unsupervised classification revealed major difficulties in identifying salinised land. While it was hoped that the natural groupings produced by unsupervised image classification would identify salinised land in the

study area, it proved impossible to isolate salinised crops from other land-cover types. The classifier could not distinguish fallow lands, fields where crops were still young, barren lands, and in some cases built-up areas from areas of stressed vegetation. Unsupervised image classification alone cannot be useful in a study to identify salinised crops.

Both the visual and digital image analysis techniques had difficulties identifying salinised lands. The inability of both techniques to differentiate salt induced stress from other forms of crop stress contributed to this difficulty. CA percentages for each image in the two techniques were used as a correction factor to estimate the amount of land identified as salinised. The statistics for this correction are tabulated in Table 6.1.

Table 6.1 Corrected estimates of potentially salinised land

Analysed image	Potentially salinised land (hectares)	Correction factor	Corrected salinised land (hectares)
Visually analysed NDVI image	179,4	0,493	88,4
Visually analysed RGB mosaicked image	208,9	0,608	127,1
Unsupervised classification of RGB Mosaicked image	1042,8	0,224	233,6
Unsupervised classification of stacked image	1245,2	0,247	307,6
Unsupervised classification of the NDVI image	1053,6	0,289	304,5
Average corrected salinised land (hectares)	212,2		
Average salinised land (%)	10,1		

On average, 212,2 hectares of a total of 2107 of irrigated land is predicted to be affected by salinisation. This constitutes about 10% of irrigated land in the study area.

6.3 RECOMMENDATIONS AND DIRECTIONS FOR FURTHER STUDY

Reversing the effects of severely salinised areas can be a very expensive and sometimes an impossible task. It is advantageous to identify salinised land before the condition becomes very severe, so that soil reclamation techniques can be implemented. This study predicted that about 10% of irrigated land in the study area is probably affected by salinisation. Farm managers should take measures to reclaim

land identified as salinised. Correct irrigation practices should be implemented to prevent further salinisation of land that is not yet salinised.

Of the two techniques employed in this study to identify salinised land, visual aerial image analysis is the one method that managed to identify a greater percentage of salinised land. However, this method could not distinguish salt stress from other types of stress. Salinised areas were identified by virtue of vegetation showing signs of stress on the imagery. This technique could have been more successful in identifying stressed crops rather identifying crops affected by a particular kind of stress. While this technique was able to identify a greater amount of salinised land, more time was spent on identifying and digitising affected areas onscreen.

Unsupervised image classification is the other technique that was tested to identify salinised land. Unsupervised classification alone could not succeed in identifying salinised areas. Coupling unsupervised classification with supervised image classification in identifying salinised land should be investigated. Also, the use of multi-date images is recommended by most authors since it helps separate land-cover types that are difficult to distinguish. In this way, temporarily fallow lands, barren lands, built areas, etc. will not be confused with stressed vegetation. Funds available to conduct this study could not permit the use of multi-date images.

Another technique that should be investigated in identifying salinised land is rule-based image classification. Using this technique, rules that will assist the classifier in classifying the image can be developed. In this way, only parts of the image that satisfy the rules will be classified. Salinised land could be relatively easier to identify in this way than by using unsupervised classification only and/or visual analysis. Rule-based image classification could not be used in this study because the images were not radiometrically calibrated as a result of non-availability of camera model information.

REFERENCES

- Allan JA 1990. Sensors, platforms and applications: acquiring and managing remotely sensed data. In Steven HD & Clark JA (eds.). *Applications of remote sensing in agriculture*, pp 1 – 17. London: Butterworths.
- Allison LE, Brown JW, Hayward HE, Richards LA, Berstein L, Fireman M, Pearson GA, Wilcox LV, Bower CA, Hatcher JT & Reeve RC 1969. *Diagnosis and improvement of saline and alkali soils*. Washington: United States Department of Agriculture.
- Arthur-Amisah-Arthur A & Miller RB 2002. Remote sensing applications in African agriculture and natural resources: Highlighting and managing the stress of increasing population pressure. *Advances in Space Research* 30, 11: 2411 – 2421.
- Armour RJ & Viljoen MF 2000. Towards quantifying the economic effects of poor and fluctuating water quality on irrigation agriculture: A case study of the lower Vaal and Riet Rivers. *Agrekon* 39, 1: 99 -111.
- Asch F & Woperecis Marco CS 2001. Responses of field-grown irrigated cultivars to varying levels of floodwater salinity in semi-arid environment. *Field Crops Research*, 70, pp 127-137.
- Blackeman RH 1990. The identification of crop diseases and stress by aerial photography. In Steven MD and Clark JA (eds.). *Applications of Remote Sensing in Agriculture*, pp 229 – 254. London: Butterworths.
- Blackmer AM & White SE 1998. Using precision farming technologies to improve management of soil and fertilizer nitrogen. *Australian Journal of Agriculture*, 49: 555 – 564.
- Boegh E, Soegaard H, Broge N, Hasager CB, Jensen NO, Schelde K & Thompson A 2002. Airborne multispectral data for quality leaf area index, nitrogen concentration, and photosynthetic efficiency in agriculture *Remote Sensing of Environment* 81: 179 – 193.
- Campbell JB 1996. *Introduction to Remote Sensing*. London: Taylor and Francis.
- Campbell JB 2002. *Introduction to Remote Sensing (3rd ed.)*. New York: The Guilford Press.
- Cassanova D, Epema GF & Goudriaan J 1998. Monitoring rice reflectance at field level for estimating biomass and LAI. *Field Crops Research*, 55: 83 - 92.

- Cuartero J & Fernandez-Munoz R 1998. Tomato and salinity. *Sciaentia Horticulturae* 78, pp 83-125.
- Curran PJ & Foody GM (eds.) 1994. *Environmental Remote Sensing from Regional to Global scales*, pp 1 – 7. New York: John Wiley and Sons.
- Dabrowska-Zielinska K, Kogan F, Ciolkosz A, Gruszczynska M & Kowalik W 2002. Modelling of crop growth conditions and crop yield in Poland using AVHRR-based indices. *International Journal of Remote Sensing*, 23, 6: 1109 – 1123.
- Department of Water Affairs and Forestry 1999. Orange River Development Project Replanning study: Water quality aspects: Orange River. Volume 1. Expected water quality.
- Dudley LM 1994. Salinity in the soil environment. In Pessarakli M (ed.). *Handbook of plant and crop stress*, pp 13-30. New York. Marcel Dekker Inc.
- ERDAS 2002. *Field guide* (6th ed.), Version 8.6 Inc. Atlanta, Georgia.
- Fitzpatrick EA 1980. *Soils: Their formation and distribution*. London: Longman.
- Francis LE & Maas EV 1994. Crop response and management on salt affected soils. In Pessarakli M(ed.). *Handbook of plant and crop stress*, pp 149 – 181. New York: Marcel Dekker Inc.
- Goel PK, Prasher SO, Landry JALandry JA, Patel RM, Patel RM, Bonnell RB, Viau AA & Miller JR 2003. Potential of airborne hyperspectral remote sensing to detect nitrogen deficiency and weed infestation in corn. *Computers and Electronics*, 38: 99 – 124.
- Greiner R 1998. Catchment management for salinity control: Model analysis for the Liverpool Plains in New South Wales. *Agricultural Systems* 56, 2, 225 – 251.
- Haboudane D, Miller JR, TrRemblay N, Zarco-Tejada PJ, Dextraze L 2002. Integrated narrow-band vegetation indices for prediction of crop chlorophyll content for application to precision agriculture. *Remote Sensing of Environment*, 81: 416 – 426.
- Hall-Konyves K 1988. Remote sensing of cultivated land. *sine loco*: Lund University Press
- Hooda RS & Dye DG 1995. Identification and mapping of irrigated vegetation using NDVI – Climatological Modelling. Global Engineering Laboratory. [Online]. Available: <http://www.gisdevelopment.net/aars/acrs> [07.08.2002].

- Jamieson PD, Martin RJ, Francis GS & Wilson DR 1995. Drought effects on biomass production and radiation use efficiency in barley. *Field Crops Research* 43: 77 – 86.
- Johnson LF, Roczen DE, Youkhana SK, Nemani RR & Bosch DF 2003. Mapping vineyard leaf area with multispectral satellite imagery. *Computers and Electronics in Agriculture*, 38: 33 – 44.
- Katerji N, Van Hoorn JW, Hamdy A & Mastrorilli M 2001. Salt tolerance of crops according to three classification methods and examination of some hypotheses about salt tolerance. *Agricultural Water Management*, 47, 1-8.
- Katerji N, van Hoorn JW, Hamdy A, Karam F & Mastrorilli M 1996. Effects of salinity on water stress, growth, and yield of maize and sunflower. *Agricultural Water Management*, 30, 237-249.
- Katerji N, van Hoorn JW, Hamdy A, Mastrorilli M 1998. Response of tomatoes, in a crop of indeterminate growth, to soil salinity. *Agricultural Water Management* 38: 59 – 68.
- Lanjeri S, Melia J & Segarra D 2001. A multi-temporal masking classification method for vineyard monitoring in central Spain. *International Journal of Remote Sensing*, 22, 16: 3167 – 3186.
- Lelong CCD, Pinet PC & Poilve H 1998. Hyperspectral imagery and stress mapping in agriculture: a case study of wheat in Bause (France). *Remote Sensing of Environment* 66: 179 – 191.
- Lenney MP, Woodstdstock CE, Collins JB & Hamdyi H 1996. The status of agricultural lands in Egypt: The use of multispectral NDVI features derived from the Landsat TM. *Remote Sensing of Environment* 56: 8 -20.
- Lewis MM 1998. Numeric classification as an aid to spectral mapping of vegetation communities. *Plant Ecology* 136: 133 - 149.
- Lillesand TM & Keifer RW 1979. *Remote sensing and image interpretation*. Toronto: John Wiley and Sons.
- Lindgren DT 1985. *Land use planning and remote sensing*. Boston: Martinus Nijhoff Publishers.
- Liu WT & Kogan F 2002. Monitoring Brazilian soybean production using NOAA/AVHRR based on vegetation condition indices. *International Journal of Remote Sensing* 23, 6: 1161 - 1179.

- Lunneta RS 1999. Applications project formulating approach. In Lunneta RS & Elvidge CD (eds.). *Remote sensing changes detection: Environmental monitoring methods and applications*, pp 1 – 15. London: Taylor and Francis.
- Maas EV, & Hoffman GJ & Asce M 1977. Crop salt tolerance - current assessment. *Journal of the Irrigation and Drainage Division*: 115 – 133.
- Mahmood K, Morris J, Collopy J & Slavicsh 2001. Groundwater uptake and sustainability of farm plantations on saline sites in Punjab province, Pakistan. *Agricultural Water Management*, 48, 1-20.
- McNairn H, Ellis J, van der Sanden JJ, Hirose T & Brown RJ 2002. Providing crop information using RADARSAT-1 and satellite optical imagery. *International Journal of Remote Sensing* 5: 851 - 870.
- Metternicht GI & Zinck JA 2003. Remote sensing of soil salinity: Potentials and constraints. *Remote Sensing of Environment* 85: 1 –20
- Moolman JH, De Clerg WP, Wessels WPJ, Meiri A & Moolman CG 1999. The use of saline water for irrigation of grapevines and development of crop salt tolerance indices. WRC Report No. 303/1/98
- Muchow RC, Robertson MJ & Pengelly BC 1993. *Field Crops Research* 32: 1 – 16.
- Mulders MA 1987. *Remote sensing in soil science*. New York. Elsevier Science Publications.
- Penuelas J, Isla R, Filella L & Araus JL 1997. Visible and Near-Infrared reflectance of salinity effects on barley. *Crop Science* 37: 198 - 202.
- Richards LA (ed.) 1954. Diagnosis and improvement of saline and alkali soils. Agricultural handbook No. 60, USDA, Washington, DC.
- Rowel DL 1994. *Soil Science: Methods and application*. London: Prince Hall
- Sahai B 1994. Remote sensing of environment: An Indian perspective. In Mehotra A & Suri RK (eds.). *Remote sensing and forest management*, pp 1 – 38. New Delhi: Indus Publishing Company.
- Sebego RJG & Arnberg W 2002. Interpretation of mopane woodlands using air photos with implications on satellite image classification. *International Journal of Applied Earth Observation and Geoinformation* 4, 2: 119 – 135.
- Slavicsh PG, Petterson GH & Griffin D 2002. Effects of irrigation water salinity and sodicity on infiltration and Lucerne growth over a shallow watertable. *Australian Journal of Experimental Agriculture* 42: 281 – 290.

- Smets SMP, Kuper M, Van Dam JC & Feddes RA 1997. Salinisation and crop transpiration of irrigated fields in Pakistan's Punjab. *Agricultural Water Management* 35: 43 – 60.
- Sommer S & Mergier JH 1988. The potential of remote sensing for monitoring rural land use changes and their effects on soil conditions. *Agriculture Ecosystems & Environment* 67: 197 – 209.
- South African Weather Service C. 1991. Climate data. [Online]. Available: <http://www.weathersa.co.za/Climat/Climstats/UpingtonStats.jsp> [04.08.2004].
- Szabolcs I 1994. Soils and salinisation. In Pessaraki M (ed.). *Handbook of Plant and Crop Stress*, pp 1-11. New York: Marcel Dekker Inc.
- Thornburn PJ, Walker GR & Jolly ID 1995. Uptake of saline groundwater by plants: An analytical model for semi-arid and arid areas. *Plant and Soil* 175: 1-11.
- Trodd NM & Dougill AJ 1998. Monitoring vegetation dynamics in semi-arid African rangelands. *Applied Geography* 18: 315 - 330.
- Uchida S 1997. Temporal analysis of agricultural land use in semi-arid tropics of India using IRS data. Japan International Research centre for Agricultural Sciences, Environmental Resource Division. [Online]. Available: <http://www.gisdevelopment.net/aars/acrs/1997/ts1007.shtml> [13.08.2002].
- Utset A & Borroto M 2001. A Modeling-GIS approach for assessing irrigation effects on soil salinisation under global warming conditions. *Agricultural Water Management* 50: 53-63.
- Van Veelen M & van Heerden JB 1998. Water Quality Aspects - Orange River Basin Volume I: Expected water quality changes. Department of Water Affairs and Forestry.
- Wang D, Poss JA, Donoavan TJ, Shannon MC & Lesch SM 2002. Biophysical properties and biomass production of elephant grass under saline conditions. *Journal of Arid Environments*, 52, 447 – 456.
- Wang D, Shannon MC & Grieve CM 2001. Salinity reduces radiation absorption and use efficiency in soybean. *Field Crops Research* 69: 267 - 277.
- Wang D, Wilson C & Shannon MC 2002. Interpretation of salinity and irrigation effects on soybean canopy reflectance in visible and near infrared spectrum domain. *International Journal of Remote Sensing* 23, 5: 811 – 824.

- Warwick NWN & Bailey PCE 1997. The effects of increasing salinity on the growth and ion content of three non-halophytic wetland macrophytes. *Aquatic Botany* 58: 73 - 88.
- White RE 1997. *Principles and practice of soil science: The soil as a natural resource*. 3rd ed. Victoria: Blackwell Science.
- Wiegand CL, Richardson AJ, Escobar DE & Gerbermann AH 1991. Vegetation indices in crop assessments. *Remote Sensing of Environment* 35: 105 - 119.
- Wienhold BJ & Trooien TP 1998. Irrigation water effects on infiltration rate in the Northern Great Plains. *Soil Science* 163, 11: 853 – 858
- William LE & Mathews MA 1990. Grape vines. In Bruce RR, Nihaus MH, Kennemasu ET & Gilley JR (eds.). *Irrigation of agricultural crops*, pp 1019 – 1048. Madison: Soil Science Society of America.
- Yehuda A & Brand A 1998. Mosaicking of orthorectified aerial images. *Photogrammetric Engineering & Remote Sensing*, 64, 2:115 – 126.
- Zhang M, Liu X & O'Neill M 2002. Spectral discrimination of *Pphytophthora infestans* infection on tomatoes based on principal component and cluster analyses. *International Journal of Remote Sensing* 23, 6: 1095-1107.
- Zietsman HL, Vlok AC, & Nel I 1998. The identification of irrigated land in an intensively cultivated area in the South Western Cape by means of satellite remote sensing. Report to the Water Research Commission by the Institute for Geographical Analysis, University of Stellenbosch. WRC Report No 440/1/96.

PERSONAL COMMUNICATIONS

- Schloms BHA 2002. Department of Geography and Environmental Studies. University of Stellenbosch. Research presentation lecture on 26 August 2002.

